Contribution from the Department of Chemistry and Laboratory for Biochemical and Genetic Engineering, William Marsh Rice University, P.O. Box 1892, Houston, Texas 77251, and Department of Chemistry, Auburn University, Auburn, Alabama 36849

Ligand Dynamics in Pentacoordinate Copper(I) and Zinc(II) Complexes[1]

DeAnna K. Coggin,[2] Jorge A. González,[2] Alan M. Kook,[2] David M. Stanbury,*[,3] and Lon J. Wilson*[,2]

Received July 3, 1990

Two new pentacoordinate zinc(II) and copper(I) complexes of the pentadentate ligand ((5-MeimidH)$_2$DAP) have been prepared and studied as their BF_4^- salts. The primary coordination sphere of each compound is composed of a central pyridine nitrogen donor atom, two imine nitrogens, and two terminal imidazole nitrogens. $[Zn^{II}((5\text{-MeimidH})_2DAP)](BF_4)_2$ has been characterized in the solid state by a single-crystal X-ray structure determination, and like its congener, $[Cu^{II}((5\text{-MeimidH})_2DAP)](BF_4)_2$, it has been found to have a geometry intermediate between idealized trigonal bipyramidal and square pyramidal. A crystal structure of the Cu(I) complex is not available, but it too is almost certainly pentacoordinate like two other closely related members of this family of Cu(I) complexes for which structures are available. Thus, the $[Cu^{I}((5\text{-MeimidH})_2DAP)]^+$ cation is the newest example of Cu(I), in a growing family of compounds, with the unusual coordination number of 5. Variable-temperature ^1H NMR spectroscopy studies in nonaqueous solvents have been used to probe intramolecular ligand dynamics for the Zn(II) and Cu(I) species in solution. In these studies, other pentacoordinate members of the family, $[M((imidH)_2DAP)]^{n+}$ (non-methylated terminal imidazole groups) and $[M((py)_2DAP)]^{n+}$ (pyridine groups replacing imidazole), have also been investigated for comparison purposes. Each of these compounds possesses two chelate rings containing dimethylene groups that undergo a dynamic exchange process leading to equivalence of the methylene protons. Coalescence rate constants have been obtained in four of the six cases. The available rate constants follow the ordering $[Zn^{II}((5\text{-MeimidH})_2DAP)]^{2+}$ (313 s^{-1}, 328 K) < $[Zn^{II}((imidH)_2DAP)]^{2+}$ (345 s^{-1}, 308 K) < $[Zn^{II}((py)_2DAP)]^{2+}$ (313 s^{-1}, 268 K) < $[Cu^{I}((py)_2DAP)]^{+}$ (303 s^{-1}, 253 K). With a coalescence temperature of ca. 203 K in CH_2Cl_2, the rate constant for $[Cu^{I}((5\text{-MeimidH})_2DAP)]^{+}$ was too large to be determined. The mechanism of exchange is believed to involve breakage of a M–N(terminal) bond, leading to optical inversion between the $\Delta(\lambda,\lambda)$ and $\Lambda(\delta,\delta)$ isomers. With two unusually long Cu–N(imine) bond distances of up to 2.4 Å, the copper(I) complexes tend more toward three coordination than do their Zn(II) counterparts, and this is reflected in their greater exchange rates. Crystal data for $[Zn^{II}((5\text{-MeimidH})_2DAP)](BF_4)_2$, $C_{21}H_{27}N_7B_2F_8Zn$: a = 18.198 (4) Å, b = 12.043 (2) Å, c = 25.506 (8) Å, β = 100.69 (3)°, Z = 8, monoclinic, space group $C2/c$. A total of 1904 unique observed data were used in the solution.

Introduction

Simple copper(I) coordination compounds with coordination numbers of 2–5 are now well documented. In general, solution-state studies of such copper(I) species have been hampered by their air sensitivity, kinetic lability, and the tendency of copper(I) to undergo disproportionation reactions. If carefully designed multidentate ligands and nonaqueous solvent media are employed, many of these disadvantages can be overcome, and we and other workers have recently exploited this strategy to examine small-molecule copper(I) chemistry in solution. Our interest in this area has largely focused on a newly emerging series of pentacoordinate copper(I) species such as the $[Cu^{I}((imidH)_2DAP)]^+$ cation:

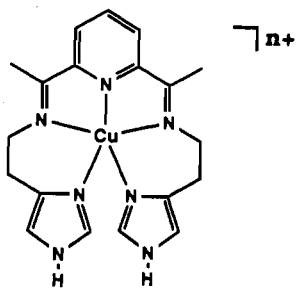

The $[Cu^{I}((imidH)_2DAP)]^+$ cation and its close structural derivatives are especially noteworthy not only because they exhibit an unusually "high" coordination number but also because crystallographic studies have established pentacoordinate structures in the solid state for both Cu(I) and Cu(II) within the same pentadentate ligand environment.[4,5] Additionally, EXAFS studies suggest that this situation is preserved in solution.[6] Thus, the $[Cu^{I,II}((imidH)_2DAP)]^{n+}$ cation couple and related systems offer an almost unique opportunity to examine coordination-number-invariant Cu(I)/Cu(II) redox chemistry in solution, and in recent work, we have initiated a series of investigations of this nature.[4-7]

The present paper continues our interest in pentacoordinate copper(I) chemistry by reporting the development and study of the $[Cu^{I}((5\text{-MeimidH})_2DAP)]^+$ cation (methyl groups at the 5-imidazole positions) and its $[M^{II}((5\text{-MeimidH})_2DAP)]^{2+}$ (M = Cu, Zn) analogue compounds. This new methyl-substituted derivative was deemed desirable to defeat a previously noted, ligand-centered isomer problem[5] and to increase compound solubility in nonaqueous solvents. Of primary concern in the current study is the first extensive analysis by NMR spectroscopy of ligand conformational dynamics for this family of labile copper(I) species. For purposes of comparison, several zinc(II) analogues have also been similarly evaluated. These studies have been performed to extend and complement our continuing electron-transfer investigations of copper(I), as reported in the following paper.[8] The application of NMR spectroscopy to the conformational analysis of metal chelates has been reviewed,[9] and the present results are some of the first such data to be obtained for Cu(I) coordination complexes of any nature.

Experimental Section

Materials. All solvents were reagent grade or better. Cyclohexane (Mallinckrodt), dimethyl sulfoxide (Mallinckrodt), methanol (Burdick & Jackson), and tetrahydrofuran (J. T. Baker) were dried by standard methods; distillation from appropriate drying agents just prior to use ensured dry solvents.[10,11] Acetonitrile (Burdick & Jackson) was purified and dried by the method of Coetzee as reported by Goodwin et al.[4,6] Purified, anhydrous methylene chloride (Mallinckrodt) was obtained by using a standard purification procedure.[11] Chloroform (Burdick & Jackson), isopropyl acetate (Aldrich), anhydrous diethyl ether (Mallinckrodt), absolute ethanol (U.S. Industrial Chemicals), and concentrated hydrochloric acid (Mallinckrodt) were used as obtained. Raney nickel (activated catalyst) was purchased from Aldrich as a slurry in

(1) Taken in part from: Coggin, D. K., PhD Dissertation, Rice University, 1990.
(2) Rice University.
(3) Auburn University.
(4) Goodwin, J. A.; Stanbury, D. M.; Wilson, L. J.; Eigenbrot, C. W.; Scheidt, W. R. *J. Am. Chem. Soc.* **1987**, *109*, 2979–2991.
(5) Goodwin, J. A.; Bodager, G. A.; Wilson, L. J.; Stanbury, D. M.; Scheidt, W. R. *Inorg. Chem.* **1989**, *28*, 35–42.
(6) Goodwin, J. A.; Wilson, L. J.; Stanbury, D. M.; Scott, R. A. *Inorg. Chem.* **1989**, *28*, 42–50.
(7) Goodwin, J. A.; Stanbury, D. M.; Wilson, L. J.; Scott, R. A. In *Biological & Inorganic Copper Chemistry*; Karlin, K. D., Zubieta, J., Eds.; Adenine Press: Guilderland, NY, 1985; pp 11–25.
(8) Coggin, D. K.; González, J. A.; Kook, A. M.; Bergman, C.; Brennan, T. D.; Scheidt, W. R.; Stanbury, D. M.; Wilson, L. J. *Inorg. Chem.*, following paper in this issue.
(9) Hawkins, C. J.; Palmer, J. A. *Coord. Chem. Rev.* **1982**, *44*, 1–60.
(10) Perrin, D. D.; Armarego, W. L. F. *Purification of Laboratory Chemicals*, 3rd ed.; Pergamon: New York, 1988.
(11) Gordon, A. J.; Ford, R. A. *The Chemist's Companion: A Handbook of Practical Data, Techniques, and References*; Wiley: New York, 1972; pp 429–436, 445–447.

0020-1669/91/1330-1115$02.50/0

water at pH 10; however, it was determined that additional activation of the catalyst was necessary.[12] 4-(Carboethoxy)-5-methylimidazole (ethyl 4-methyl-5-imidazolecarboxylate), 2,6-diacetylpyridine, and $LiAlH_4$ were purchased from Aldrich, $Zn^{II}(BF_4)_2 \cdot 6H_2O$ and $Cu^{II}(BF_4)_2 \cdot 3H_2O$ were purchased from Alfa, hydrogen, prepurified nitrogen, argon, and anhydrous ammonia gases were purchased from Big Three Industries, and NaCN was purchased from J. T. Baker.

Column separations employed the use of a chromatographic column (Ace Glass) equipped with a Teflon coupling, a Teflon Luer drip adapter, and a feed tube. Silica gel was dried in an oven at 135 °C for a minimum of 6 h and then cooled to room temperature under vacuum in a desiccator prior to packing the column. The potentiostat and coulometer used for the synthesis of $[Cu^{I}((5\text{-MeimidH})_2DAP)](BF_4)$ and $[Cu^{I}(imidH)_2DAP)](BF_4)$ were Princeton Applied Research Models 371 and 379, respectively. Current amplitude was monitored with an Industrial Scientific Omniscribe strip chart recorder. Coulometry employed background compensation available on the PAR Model 379 instrument.

Syntheses. 5-Methylhistamine was synthesized according to a modified method of Durant et al.[13] During this procedure, three intermediates were isolated: 5-methyl-4-(hydroxymethyl)imidazole hydrochloride, 5-methyl-4-(chloromethyl)imidazole hydrochloride, and 5-methyl-4-(cyanomethyl)imidazole. Synthetic procedures for these intermediates are given directly below.

5-Methyl-4-(hydroxymethyl)imidazole Hydrochloride. $LiAlH_4$ (5.6 g, 0.15 mol) was added portionwise to a stirred suspension of 4-(carboethoxy)-5-methylimidazole (15.4 g, 0.10 mol) in dry THF (1 L) at room temperature. Concentrated hydrochloric acid (≈25 mL) was added dropwise to the grey suspension. During the addition, a sticky gray solid settled to the bottom of the flask. The mother liquor (pH 6) was removed by decantation. Extraction of the gray powder with absolute ethanol (≈200 mL) gave a pale yellow filtrate. Celite was used to aid filtration of the alcoholic solution. Anhydrous diethyl ether was added to the filtrate until turbidity persisted. The flask was sealed with a cork stopper and placed in the freezer overnight, during which time a solid volunteered from solution. The white powder was collected by suction filtration, washed with anhydrous diethyl ether, and dried under vacuum at room temperature for 12 h. Yield: 12.24 g (82%). Mp: 235–240 °C (lit. 240–242 °C).[13] ^1H NMR (90 MHz, D_2O, DSS internal reference): δ = 2.20 (s, imidazole CH_3), δ = 4.53 (s, CH_2), δ = 8.41 (s, imidazole H).

5-Methyl-4-(chloromethyl)imidazole Hydrochloride. 5-Methyl-4-(hydroxymethyl)imidazole hydrochloride (12.0 g, 0.08 mol) was added portionwise with stirring to $SOCl_2$ (50 ml) at room temperature. The cream-colored solution was heated to between 60 and 70 °C by an oil bath for 2 h before the solvent was removed via vacuum distillation. Caution was exercised during solvent removal to avoid charring of the residual solid. The cream-colored solid was dissolved in absolute ethanol (100 mL). Activated carbon was added to the solution, and the mixture was heated to boiling and gravity filtered; a precipitate formed as the pale yellow filtrate cooled to room temperature. The flask was sealed and placed in the freezer for a few hours to promote additional solid formation, and the product was isolated by suction filtration, washed with anhydrous diethyl ether, and dried under vacuum at room temperature overnight. Initially, 5.82 g of a white powder was recovered, and an additional 3.85 g was obtained by adding anhydrous diethyl ether to the filtrate. Again, the mixture was allowed to stand in the freezer for several hours before the solid was collected. Total yield: 9.67 g (71%). Mp: 220–222 °C (lit. 222 °C).[13] ^1H NMR (90 MHz, D_2O, DSS internal reference): δ = 2.14 (s, imidazole CH_3), δ = 4.47 (s, CH_2), δ = 8.36 (s, imidazole H).

5-Methyl-4-(cyanomethyl)imidazole. 5-Methyl-4-(chloromethyl)-imidazole hydrochloride (8.9 g, 0.05 mol) was added portionwise over a period of 10 min to a stirred mixture of NaCN (14.7 g, 0.30 mol) in dry DMSO (0.1 L). The yellow reaction mixture was heated to 50 °C and allowed to stir for 1 h. Removal of the solvent by vacuum distillation gave a dark brown residue, which was then dissolved in deionized water (≈100 mL). Continuous extraction of the aqueous solution with isopropyl acetate (≈400 mL) gave a dark brown solution, to which was added activated carbon. Gravity filtration and removal of the solvent under reduced pressure gave a pale yellow powder. The solid was dried in vacuo at room temperature for 24 h. Yield: 2.37 g (36%). Mp: 162–163 °C (lit. 163–164 °C).[13] ^1H NMR (90 MHz, D_2O, DSS internal reference): δ = 2.06 (s, imidazole CH_3), δ = 3.64 (s, CH_2), δ = 7.47 (s, imidazole H). Mass spectrometry: 121 $(M)^+$, 122 $(M + 1)^+$.

5-Methylhistamine. In an autoclave cooled by a dry ice/2-propanol bath, 5-methyl-4-(cyanomethyl)imidazole (2.1 g, 0.02 mol) and a catalytic amount of activated Raney nickel were added to a solution of absolute ethanol (75 mL) saturated with anhydrous ammonia. The autoclave was sealed and pressurized with H_2 gas to 1050 psi. Hydrogenation was carried out at 160 °C and 1500 psi for 4 h with constant stirring using a Teflon-coated stir bar. After cooling to room temperature, the reaction mixture was gravity filtered before the solvent was removed under reduced pressure. Partial purification of the crude product was accomplished by dissolving the dark brown oil in chloroform (250 mL), adding activated carbon to the solution, and warming the mixture to boiling. The hot suspension was gravity filtered, and removal of the solvent under reduced pressure gave a pale yellow oil that was then dried under vacuum at room temperature for 12 h. Yield: 1.88 g (87%). ^1H NMR (90 MHz, $CDCl_3$, TMS internal reference): δ = 2.14 (s, imidazole CH_3), δ = 2.64 (m, CH_2), δ = 2.90 (m, CH_2), δ = 5.28 (broad s, NH_2), δ = 7.32 (s, imidazole H). Mass spectrometry: 125 $(M)^+$, 126 $(M + 1)^+$.

$[Zn^{II}((5\text{-MeimidH})_2DAP)](BF_4)_2$. A ligand solution was prepared according to the general procedure of Simmons et al.[14] 5-Methylhistamine (0.628 g, 5.0 mmol) and 2,6-diacetylpyridine (0.422 g, 2.6 mmol) were dissolved in dry methanol (20 mL). The solution was refluxed over molecular sieves (Linde, 4-Å porosity) for 1 h. $Zn^{II}(BF_4)_2 \cdot 6H_2O$ (1.109 g, 3.2 mmol) in methanol (20 mL) was added dropwise to the room-temperature ligand solution by using an addition funnel. The reaction mixture was gently swirled for another 10 min, gravity filtered, and reduced to dryness under reduced pressure at room temperature. The pale yellow solid was dried in vacuo at room temperature overnight and then purified by recrystallization from acetonitrile/diethyl ether. Due to the hygroscopic nature of the compound, fairly dry samples were obtained only after they were dried in vacuo over P_2O_5 at 78 °C for several days. Anal. Calcd for $C_{21}H_{27}N_7B_2F_8Zn \cdot 1.5H_2O$: C, 39.20; H, 4.70; N, 15.24; Zn, 10.16. Found: C, 39.44; H, 4.22; N, 15.43; Zn, 10.04. UV–vis (CH_3CN; λ_{max}, nm (ϵ, M^{-1} cm^{-1})): 296 (3850). ^1H NMR at 293 K (300 MHz, CD_3CN internal reference, δ = 1.93; see Figure 1a for the proton-labeling scheme and spectrum): δ = 10.68 (broad s, imidazole NH), δ = 8.47 (t, H8), δ = 8.29 (d, H7,9), δ = 7.78 (s, H2,2′), δ = 4.14 (broad m, equatorial Hα,α'), δ = 3.70 (broad m, axial Hα,α'), δ = 3.05 (m, Hβ,β'), δ = 2.49 (s, Me6,10), δ = 2.19 (s, Me5,5′). A crystal structure of this new Zn(II) compound is reported below.

$[Zn^{II}((imidH)_2DAP)](BF_4)_2$. A ligand solution was prepared according to the method of Merrill et al.[15] except that $Zn^{II}(BF_4)_2 \cdot 6H_2O$ in CH_3OH (20 mL) was added dropwise to the cooled ligand solution rather than as a solid. All subsequent manipulations were identical with the method of Merrill et al. Elemental analyses (C, H, N) were as satisfactory as previously reported.[15] ^1H NMR at 293 K (300 MHz, CD_3CN internal reference, δ = 1.93; see Figure 1b for the proton-labeling scheme and spectrum): δ = 10.93 (broad s, imidazole NH), δ = 8.48 (t, H8), δ = 8.30 (d, H7,9), δ = 7.92 (s, H2,2′), δ = 7.10 (s, H5,5′), δ = 4.16 (broad m, equatorial Hα,α'), δ = 3.74 (broad m, axial Hα,α'), δ = 3.14 (m, Hβ,β'), δ = 2.45 (s, Me6,10).

$[Zn^{II}((py)_2DAP)](BF_4)_2$. A ligand solution was prepared according to the method of Merrill et al.[15] except that $Zn^{II}(BF_4)_2 \cdot 6H_2O$ was added as a solution in MeOH dropwise to the cooled ligand solution rather than as a solid. All subsequent manipulations were identical with the method of Merrill et al. Elemental analyses (C, H, N) were as satisfactory as previously reported.[15] ^1H NMR at 293 K (300 MHz, CD_3CN internal reference, δ = 1.93; see Figure 1c for the proton-labeling scheme and spectrum): δ = 8.49 (t, H8), δ = 8.43 (d, H2,2′), δ = 8.32 (d, H7,9), δ = 8.10 (t, H3,3′), δ = 7.67 (d, H5,5′), δ = 7.55 (t, H4,4′), δ = 4.16 (broad s, Hα,α'), δ = 3.40 (m, Hβ,β'), δ = 2.54 (s, Me6,10).

$[Cu^{II}((5\text{-MeimidH})_2DAP)](BF_4)_2$. A ligand solution was prepared according to the general procedure of Simmons et al.[14] 5-Methylhistamine (0.26 g, 2.1 mmol) and 2,6-diacetylpyridine (0.17 g, 1.0 mmol) were dissolved in dry methanol (15 mL). The solution was refluxed over molecular sieves (Linde, 4-Å porosity) for 1 h. $Cu^{II}(BF_4)_2 \cdot 3H_2O$ (0.32 g, 1.1 mmol) in methanol (10 mL) was added dropwise to the room-temperature ligand solution by using an addition funnel. The reaction mixture was gently swirled for another 10 min, gravity filtered, and reduced to dryness under reduced pressure at room temperature. Usually, the dark green solid residue was dried in vacuo at room temperature overnight, but due to the hygroscopic nature of the pure compound, very dry solids were obtained only after drying in vacuo over P_2O_5 at 78 °C for at least 3 days. Purification of $[Cu^{II}((5\text{-MeimidH})_2DAP)](BF_4)_2$ was accomplished by low-pressure column chromatography. For a typical

(12) Mozingo, R. In *Organic Synthesis*; Horning, E. C., Allen, C. F. H., Drake, N. L., Hamilton, C. S., Shriner, R. L., Smith, L. I., Snyder, H. R., Eds.; Wiley: New York, 1955; Collect. Vol. III, pp 181–183.
(13) Durant, G. J.; Emmett, J. C.; Ganellin, C. R.; Roe, A. M.; Slater, R. A. *J. Med. Chem.* **1976**, *19*, 923–928.
(14) Simmons, M. G.; Merrill, C. L.; Wilson, L. J.; Bottomley, L. A.; Kadish, K. M. *J. Chem. Soc., Dalton Trans.* **1980**, 1827–1837.
(15) Merrill, C. L.; Wilson, L. J.; Thamann, T. J.; Loehr, T. M.; Ferris, N. S.; Woodruff, W. H. *J. Chem. Soc., Dalton Trans.* **1984**, 2207–2221.

separation, the crude product from the reaction mixture (120–160 mg) was dissolved in dry CH_3CN (≈2 mL), and the dark-brown green solution was pipetted onto a column of silica gel (length 365–395 mm, diameter 15 mm). The sample was eluted with acetonitrile at low pressure. As the sample traveled down the column, several bands were obtained: green, red-violet, olive-green, and brown (or dark green-brown), in order from bottom to top. Only the middle portion of the green band was collected. A green powder (35–50 mg) was obtained after evaporation of the solution, and it was subsequently dried in vacuo at room temperature. Total yield: 0.12 g (17%). Anal. Calcd for $C_{21}H_{27}N_7B_2F_8Cu\cdot 5H_2O$: C, 35.79; H, 5.29; N, 13.91; Cu, 9.02. Found: C, 35.33; H, 3.94; N, 14.46; Cu, 8.47. A crystal structure of this new Cu(II) compound is reported elsewhere.[8]

$[Cu^I((5\text{-MeimidH})_2DAP)](BF_4)$. Solutions of the O_2-sensitive Cu(I) compound were prepared under argon by controlled-potential, bulk electrolysis of the analogous Cu(II) compound by using a cell with Schlenk-line connections.[4,6] Typically Cu(II) (40–80 μmol) in acetonitrile solution, with 0.05 M $NaBF_4$ as supporting electrolyte, was reduced by a platinum-gauze working electrode held at a potential 230 mV cathodic of the reversible potential for 4–6 h. A platinum-wire auxilary electrode and a Ag/AgCl reference electrode, both separated from the bulk solution by fritted-glass tubes containing electrolyte solution, completed the three-electrode geometry. The end point of the electrolysis was determined by little or no current flow. When a reduction was judged complete, the red solution was transferred to an evacuated Schlenk flask prior to removing the solvent under vacuum. The Cu(I) complex was extracted by washing with dry, deoxygenated methylene chloride. All CH_2Cl_2 filtrates were reduced to dryness under vacuum. A hygroscopic red-brown powder was obtained by adding cyclohexane (100 mL) to an CH_3CN/CH_2Cl_2 (5 mL/100 mL) solution of the Cu(I) complex. Anal. Calcd for $C_{21}H_{27}N_7BF_4Cu\cdot CH_2Cl_2$: C, 43.31; H, 4.77; N, 16.00; Cu, 10.37. Found: C, 43.17; H, 4.42; N, 15.34; Cu, 10.43. ^1H NMR at 293 K (300 MHz, CD_3CN internal reference, $\delta = 1.93$, see Figure 2 for the proton-labeling scheme and spectrum): $\delta = 10.01$ (broad s, imidazole NH), $\delta = 8.06$ (t, H8), $\delta = 7.99$ (d, H7,9), $\delta = 7.34$ (s, H2,2′), $\delta = 3.87$ (broad m, Hα,α′), $\delta = 3.17$ (broad m, Hβ,β′), $\delta = 2.25$ (s, Me6,10), $\delta = 2.14$ (s, Me5,5′).

$[Cu^I((imidH)_2DAP)](BF_4)$. $[Cu^I((imidH)_2DAP)](BF_4)$ was prepared and isolated by the method of Goodwin et al.[4,6] Elemental analysis (C, H, N, Cu) were as satisfactory as previously reported results.[14,15] ^1H NMR at 293 K (300 MHz, CD_3CN internal reference, $\delta = 1.93$; see Figure 1b for the proton-labeling scheme): $\delta = 10.14$ (broad s, imidazole NH), $\delta =$ [8.15–7.81] (broad m, H8 and H7,9), $\delta = 7.48$ (s, H2,2′), $\delta = 6.87$ (s, H5,5′), $\delta = 3.88$ (broad m, Hα,α′), $\delta = 3.22$ (broad m, Hβ,β′), $\delta = 2.27$ (s, Me6,10).

Physical and Spectroscopic Measurements. Mass spectra of 5-methylhistamine and its precursors were obtained on a Finnigan 9500 automated gas chromatograph/mass spectrometer. Proton NMR spectra were obtained at 90 MHz on a JEOL FX90Q NMR spectrometer and at 300 MHz on an IBM/Bruker AF-300 NMR spectrometer. Chloroform-d_1 (Aldrich) and D_2O (Sigma), obtained as 99.8 atom % D solvents, were used in studies of 5-methylhistamine and its precursors, while acetonitrile-d_3 (Aldrich), dichloromethane-d_2 (Aldrich), and acetone-d_6 (Cambridge Isotope Laboratories) were used in studies of the metal compounds. Tetramethylsilane (TMS) and sodium 2,2-dimethyl-2-silapentane-5-sulfonate (DSS) served as internal standards for the studies in $CDCl_3$ and D_2O, respectively. UV–vis spectra were obtained on a Cary 17 spectrophotometer using matched quartz cells. Elemental analyses were performed by Galbraith Laboratories, Inc., Knoxville, TN.

Crystal Growth and Data Collection. Crystals of $[Zn^{II}((5\text{-MeimidH})_2DAP)](BF_4)_2$ suitable for X-ray diffraction were grown in the freezer by slow vapor diffusion of anhydrous diethyl ether into dilute acetonitrile solutions of the salt.

A clear, needle-shaped crystal with approximate dimensions of 0.25 × 0.25 × 0.70 mm^3 was mounted on the tip of a glass fiber with epoxy cement. All measurements on the crystal were performed at room temperature (23 °C). Preliminary crystal examination and data collection were performed with graphite-monochromated Mo Kα radiation ($\bar{\lambda}$ = 0.71073 Å). The cell constants and orientation matrix for data collection were derived from a least-squares refinement of 50 reflections ($6 \le 2\theta \le 15$).

Intensity data were collected (ω scans) by using a Rigaku AFC5S automated four-circle diffractometer [Rigaku CRYSTAN/TEXTL (4) automatic data collection series (Molecular Structure Corp.)][16] through the *hkl* range 0 to 24, 0 to 16, and −33 to 33, respectively, with 6162 reflections measured, 5953 independent reflections processed, 1904 reflections observed ($I > 3.0\sigma(I)$), and $2\theta_{max} = 55°$. Three standards were measured every 150 reflections, showing essentially no decay in intensity (average percent change was 0.1%). The data were corrected for absorption (ψ-scan) and Lorentz–polarization effects.

Table I. Summary of Crystal Data and Intensity Collection Parameters for $[Zn^{II}((5\text{-MeimidH})_2DAP)](BF_4)_2$

T, °C	23	d(calcd), g/cm³	1.49
formula	$C_{21}H_{27}N_7B_2F_8Zn$		
fw	616.48	radiation	Mo Kα ($\bar{\lambda}$ = 0.71073 Å) graphite-monochromated)
space group	$C2/c$		
cryst syst	monoclinic	diffractometer	Rigaku AFC5S
a, Å	18.198 (4)	scan technique	ω
b, Å	12.046 (2)	no. of unique obsd data	1904
c, Å	25.506 (8)		
β, deg	100.69 (3)	no. of variables	305
V, Å³	5493 (2)	residuals	$R_1 = 0.075$
Z	8		$R_2 = 0.089$
		data/param	6.3

Table II. Fractional Coordinates for $[Zn^{II}((5\text{-MeimidH})_2DAP)](BF_4)_2$

atom	x	y	z
Zn	0.00927 (7)	0.2091 (1)	0.60919 (4)
N(1)	0.0273 (5)	0.3535 (7)	0.6472 (3)
C(2)	0.0142 (6)	0.457 (1)	0.6322 (4)
N(3)	0.0473 (5)	0.5258 (7)	0.6710 (4)
C(4)	0.0834 (6)	0.462 (1)	0.7129 (4)
C(5)	0.1258 (7)	0.512 (1)	0.7642 (5)
C(6)	0.0720 (6)	0.354 (1)	0.6973 (4)
C(7)	0.1020 (6)	0.2499 (9)	0.7245 (4)
C(8)	0.1600 (6)	0.192 (1)	0.6977 (4)
N(9)	0.1267 (4)	0.1734 (6)	0.6408 (3)
C(10)	0.1669 (6)	0.156 (1)	0.6068 (4)
C(11)	0.2506 (7)	0.149 (1)	0.6164 (5)
C(12)	0.1255 (6)	0.1451 (9)	0.5510 (4)
C(13)	0.1565 (6)	0.116 (1)	0.5061 (5)
C(14)	0.1095 (7)	0.114 (1)	0.4564 (4)
C(15)	0.0359 (7)	0.139 (1)	0.4511 (5)
C(16)	0.0079 (6)	0.1639 (9)	0.4958 (4)
N(17)	0.0528 (5)	0.1652 (7)	0.5440 (3)
C(18)	−0.0723 (6)	0.1858 (8)	0.4991 (4)
C(19)	−0.1289 (7)	0.178 (1)	0.4484 (4)
N(20)	−0.0864 (4)	0.2134 (8)	0.5441 (3)
C(21)	−0.1617 (6)	0.228 (1)	0.5526 (4)
C(22)	−0.1627 (5)	0.230 (1)	0.6125 (4)
C(23)	−0.1291 (5)	0.1272 (8)	0.6400 (4)
C(24)	−0.1611 (6)	0.0419 (9)	0.6618 (4)
C(25)	−0.2397 (6)	0.017 (1)	0.6661 (4)
N(26)	−0.1036 (5)	−0.0284 (7)	0.6829 (3)
C(27)	−0.0397 (6)	0.016 (1)	0.6721 (4)
N(28)	−0.0527 (4)	0.1096 (7)	0.6469 (3)

Crystal Structure Determination. The structure was solved by using the direct methods programs MITHRIL[17] to find the heavy atom and DIRDIF[18] to find all of the remaining non-hydrogen atoms. Idealized hydrogen atom positions (C–H = 0.95 Å) were calculated and refined with isotropic temperature factors in the final stages of structure refinement. Because the BF_4^- ions were poorly defined, they were treated as rigid groups. The ratio of the occupancies for the disordered groups was set to 24/76 (starred/nonstarred) for one BF_4^- ion and 42/58 for the other ion. The final model (based on 1904 observed reflections and 305 variable parameters) converged with $R_1 = 0.075$ and $R_2 = 0.089$ and a data/variables ratio of 6.3.[19] Table I summarizes the data collection parameters, while atomic coordinates are listed in Table II. Additional crystallographic data are available in the supplementary material.

Variable-Temperature NMR Measurements. Temperature-dependent ^1H NMR measurements were performed on an IBM/Bruker AF-300 NMR spectrometer with a variable-temperature controller. NMR spectra were obtained at various temperatures, and typically, a FID consisted of 128, 32 K scans. Studies of the Zn(II) compounds were performed in CD_3CN over a temperature range of 243–343 K and in acetone-d_6 over a range of 203–283 K. Measurements were made at 10 or 20° intervals, which leads to the ±5 or 10° uncertainty in the coalescence temperatures. Spectra of $[Zn^{II}((5\text{-MeimidH})_2DAP)]^{2+}$ in

(16) All calculations in this crystal structure study were performed by using the TEXSAN crystallographic software package of Molecular Structure Corp.

(17) Gilmore, C. J. *J. Appl. Crystallogr.* **1984**, *17*, 42–46.
(18) Beurskens, P. T. DIRDIF. Technical Report 1984/1; Crystallography Laboratory: Toernooiveld, 6525 Ed Nijmegen, Netherlands.
(19) $R_1 = \sum||F_o| - |F_c||/\sum|F_o|$ and $R_2 = [\sum(|F_o| - |F_c|)^2/\sum w(F_o)^2]^{1/2}$.

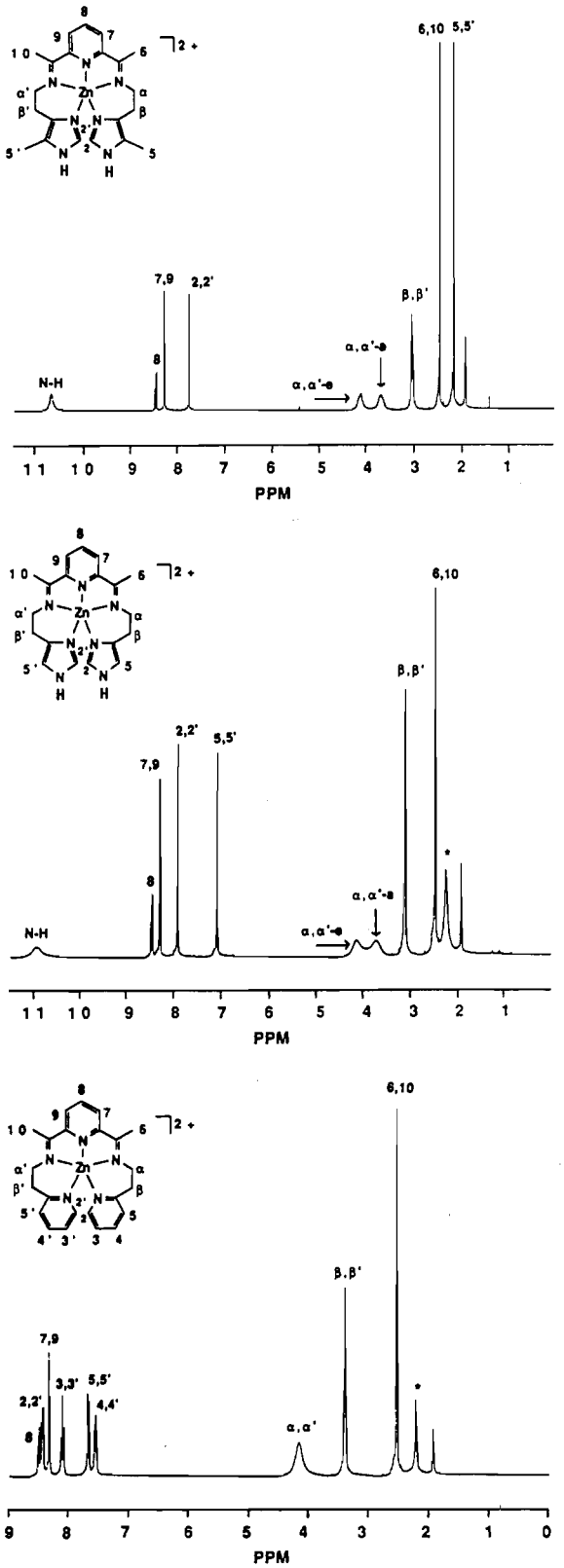

Figure 1. 300-MHz ^{1}H NMR spectra in CD_3CN at 293 K. (a, top) $[Zn^{II}((5\text{-MeimidH})_2DAP)]^{2+}$, ($\alpha,\alpha'$-a) methylene proton with an axial orientation, (α,α'-e) methylene proton with an equatorial orientation; (b, middle) $[Zn^{II}((imidH)_2DAP)]^{2+}$, ($\alpha,\alpha'$-a) methylene proton with an axial orientation, (α,α'-e) methylene proton with an equatorial orientation, (*) H_2O signal; (c, bottom) $[Zn^{II}((py)_2DAP)]^{2+}$, (*) H_2O signal.

CD_3CN came from two separate samples, each approximately 10 mM in the Zn(II) compound. The first sample provided spectral data over a range of 243–323 K, while the second sample covered a range of 323–343 K.

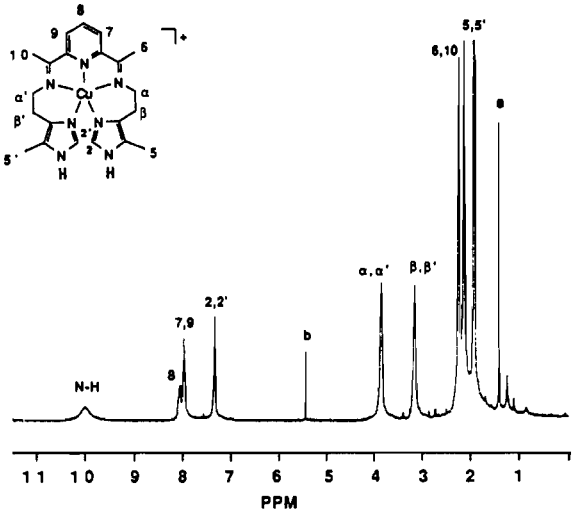

Figure 2. 300-MHz ^{1}H NMR spectrum of $[Cu^I((5\text{-MeimidH})_2DAP)]^+$ in CD_3CN at 22 °C. Extraneous peaks are labeled as followed: (a) contaminant cyclohexane; (b) contaminant CH_2Cl_2. Both a and b are from the drybox atmosphere.

CD_3CN and CD_2Cl_2 were used in studies of the analogous Cu(I) compounds. Because solutions of these compounds are extremely O_2-sensitive, the solvents were deoxygenated by the freeze–pump–thaw method on a Schlenk-line prior to sample preparation. Samples of $[Cu^I((5\text{-MeimidH})_2DAP)]^+$ and $[Cu^I((imidH)_2DAP)]^+$ were prepared in a Vacuum Atmospheres drybox under a N_2 atmosphere and then carefully sealed with a rubber septum and Parafilm to prevent air oxidation. Studies in CD_3CN covered a temperature range of 243–293 K, while those in CD_2Cl_2 covered a range of 193–283 K.

The lower limit of the temperature range was governed by properties of the NMR sample. The low-temperature measurements were terminated when the line shapes of the spectrum were significantly influenced by the increased viscosity of the sample.

Chemical shifts are reported in parts per million (ppm). The chemical shift of residual solvent served as an internal reference and was set to 1.93 ppm for CD_3CN, 2.05 ppm for acetone-d_6, and 5.32 ppm for CD_2Cl_2.

The methylene proton region of the spectra for $[Zn^{II}((5\text{-MeimidH})_2DAP)]^{2+}$ in CD_3CN was analyzed, to a first approximation, by using the computer program PANIC;[20] calculations were performed on the ASPECT 3000 computer of the IBM/Bruker AF-300 spectrometer. Because a rigorous analysis of the spin system was beyond the scope of this study, the iterative feature of the program was not used. The chemical shift differences and coupling constants of the dimethylene protons, initially obtained as estimates from the experimental data, were manually adjusted and ultimately gave excellent agreement with the observed spectra at the lower temperatures, thus permitting assignment of the proton resonances.

Results

This paper reports the synthesis and characterization of the new $[Zn^{II}((5\text{-MeimidH})_2DAP)](BF_4)_2$ compound, as well as the temperature-dependent ^{1}H NMR spectra of it and related Zn(II) and Cu(I) compounds. The pentadentate ligand (5-MeimidH)$_2$DAP is derived by a Schiff-base condensation of 5-methylhistamine with 2,6-diacetylpyridine in methanol,[14,15] and subsequent addition of $Zn^{II}(BF_4)_2 \cdot 6H_2O$ yields the pentacoordinate compound. Results from a single-crystal X-ray structure determination of the $[Zn^{II}((5\text{-MeimidH})_2DAP)]^{2+}$ cation are presented below. Syntheses and characterization of $[Zn^{II}((imidH)_2DAP)](BF_4)_2$ and $[Zn^{II}((py)_2DAP)](BF_4)_2$ have been reported elsewhere.[15] $[Zn^{II}((5\text{-MeimidH})_2DAP)](BF_4)_2$ is the seventh member in a series of pentacoordinate Zn(II) compounds studied by our group; the other members of this series have also been thoroughly characterized, and analyses of the data have been reported.[14,15] The Cu(II) and Cu(I) analogues of $[Zn^{II}((5\text{-MeimidH})_2DAP)](BF_4)_2$ are also new members of our series of

(20) PANIC: Parameter Adjustment in NMR by Iteration Calculation. PANIC is a minicomputer version of the Laocoon-type programs used in large computer systems and is available in the ASPECT 3000 Computer Program Library.

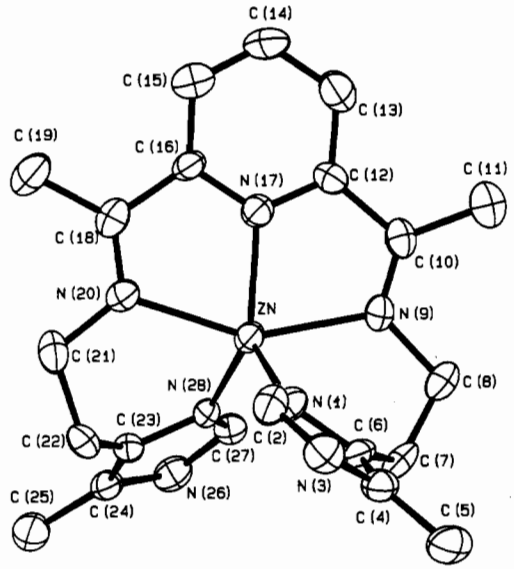

Figure 3. ORTEP drawing of the $[Zn^{II}((5\text{-MeimidH})_2DAP)]^{2+}$ cation with the atom-labeling scheme. Ellipsoids are contoured at the 50% level.

Table III. Selected Bond Distances (Å) in $[Zn^{II}((5\text{-MeimidH})_2DAP)](BF_4)_2$[a]

Zn–N(1)	1.990 (9)	C(12)–N(17)	1.32 (1)
Zn–N(9)	2.182 (8)	C(13)–C(14)	1.39 (2)
Zn–N(17)	2.039 (9)	C(14)–C(15)	1.36 (2)
Zn–N(20)	2.171 (7)	C(15)–C(16)	1.36 (2)
Zn–N(28)	2.009 (8)	C(16)–N(17)	1.35 (1)
N(1)–C(2)	1.32 (2)	C(16)–C(18)	1.50 (2)
N(1)–C(6)	1.38 (1)	C(18)–C(19)	1.50 (1)
C(2)–N(3)	1.34 (1)	C(18)–N(20)	1.27 (1)
N(3)–C(4)	1.38 (1)	N(20)–C(21)	1.44 (1)
C(4)–C(5)	1.52 (2)	C(21)–C(22)	1.53 (2)
C(4)–C(6)	1.36 (2)	C(22)–C(23)	1.50 (1)
C(6)–C(7)	1.49 (1)	C(23)–C(24)	1.35 (1)
C(7)–C(8)	1.53 (2)	C(23)–N(28)	1.39 (1)
C(8)–N(9)	1.48 (1)	C(24)–C(25)	1.48 (2)
N(9)–C(10)	1.25 (1)	C(24)–N(26)	1.38 (1)
C(10)–C(11)	1.50 (2)	N(26)–C(27)	1.35 (1)
C(10)–C(12)	1.49 (1)	C(27)–N(28)	1.30 (1)
C(12)–C(13)	1.41 (2)		

[a] Estimated standard deviations in the least significant figure are given in parentheses.

pentacoordinate copper compounds,[7,14,15] and a discussion of their spectroscopic properties, as well as the X-ray crystal structure of $[Cu^{II}((5\text{-MeimidH})_2DAP)]^{2+}$, appears in the subsequent paper.[8]

Crystal Structure Determination. An overall perspective of the $[Zn^{II}((5\text{-MeimidH})_2DAP)]^{2+}$ cation, as given in Figure 3, illustrates the atom-labeling scheme. Individual values of bond distances and angles are given in Tables III and IV, respectively. The coordination sphere of the $[Zn^{II}((5\text{-MeimidH})_2DAP)]^{2+}$ cation is probably best described as a distorted trigonal bipyramid with the two imidazole nitrogen atoms and the pyridine nitrogen atom defining the trigonal plane. All three angles in this plane are close to the ideal 120°; N(1)–Zn–N(17) and N(28)–Zn–N(17) are 124.6 (4) and 125.1 (4)°, respectively, while N(1)–Zn–N(28) is 110.2 (4)°. In contrast, the angle involving the "axial" imine nitrogen atoms, is 151.4 (4)°, significantly less than the ideal value of 180°. The average Zn–N bond distance to the three trigonal donor atoms is 2.02 (1) Å, whereas the average bond distance to the two axial donor atoms is longer at 2.18 (1) Å. The pyridyl ring and the two imine bonds (DAP: N(9)–N(20)) are coplanar, and both imidazole rings (imidH(1), N(1)–C(6) excluding C(5), and imidH(2), C(23)–N(28) excluding C(25)) are also planar; average displacements from the least-squares planes are 0.0487, 0.0058, and 0.0056 Å, respectively. Although the complex has no crystallographically imposed symmetry, it does have approximate C_2 symmetry, with the C_2 axis passing through the central pyridine and the Zn atom. Selected least-squares planes and a packing diagram are available in the supplementary material.

Table IV. Selected Bond Angles (deg) in $[Zn^{II}((5\text{-MeimidH})_2DAP)](BF_4)_2$[a]

N(1)–Zn–N(9)	86.0 (3)	C(10)–C(12)–C(13)	126.3 (9)
N(1)–Zn–N(17)	124.8 (3)	C(10)–C(12)–N(17)	115.3 (9)
N(1)–Zn–N(20)	112.9 (3)	C(13)–C(12)–N(17)	118.5 (9)
N(1)–Zn–N(28)	110.1 (3)	C(12)–C(13)–C(14)	118 (1)
N(9)–Zn–N(17)	75.4 (3)	C(13)–C(14)–C(15)	121 (1)
N(9)–Zn–N(20)	151.4 (3)	C(14)–C(15)–C(16)	119 (1)
N(9)–Zn–N(28)	107.7 (3)	C(15)–C(16)–N(17)	121 (1)
N(17)–Zn–N(20)	76.1 (3)	C(15)–C(16)–C(18)	127.1 (9)
N(17)–Zn–N(28)	125.0 (3)	N(17)–C(16)–C(18)	112.2 (9)
N(20)–Zn–N(28)	86.5 (3)	Zn–N(17)–C(12)	117.9 (6)
Zn–N(1)–C(2)	133.1 (7)	Zn–N(17)–C(16)	119.2 (7)
Zn–N(1)–C(6)	118.1 (7)	C(12)–N(17)–C(16)	122.8 (9)
C(2)–N(1)–C(6)	108.0 (9)	C(16)–C(18)–C(19)	117.3 (9)
N(1)–C(2)–N(3)	109.6 (9)	C(16)–C(18)–N(20)	117.3 (8)
C(2)–N(3)–C(4)	108.1 (9)	C(19)–C(18)–N(20)	125 (1)
N(3)–C(4)–C(5)	123 (1)	Zn–N(20)–C(18)	114.8 (7)
N(3)–C(4)–C(6)	106.3 (8)	Zn–N(20)–C(21)	122.7 (6)
C(5)–C(4)–C(6)	131 (1)	C(18)–N(20)–C(21)	121.7 (8)
N(1)–C(6)–C(4)	107.9 (9)	N(20)–C(21)–C(22)	109.8 (8)
N(1)–C(6)–C(7)	122.0 (9)	C(21)–C(22)–C(23)	111.8 (9)
C(4)–C(6)–C(7)	130.0 (8)	C(22)–C(23)–C(24)	130.8 (9)
C(6)–C(7)–C(8)	113.4 (9)	C(22)–C(23)–N(28)	119.9 (9)
C(7)–C(8)–N(9)	108.5 (8)	C(24)–C(23)–N(28)	109.3 (8)
Zn–N(9)–C(8)	121.7 (7)	C(23)–C(24)–C(25)	133 (1)
Zn–N(9)–C(10)	115.8 (6)	C(23)–C(24)–N(26)	105.9 (9)
C(8)–N(9)–C(10)	121.2 (8)	C(25)–C(24)–N(26)	122 (1)
N(9)–C(10)–C(11)	127 (1)	C(24)–N(26)–C(27)	107.4 (8)
N(9)–C(10)–C(12)	114.9 (9)	N(26)–C(27)–N(28)	111.0 (9)
C(11)–C(10)–C(12)	118 (1)		

[a] Estimated standard deviations in the least significant figure are given in parentheses.

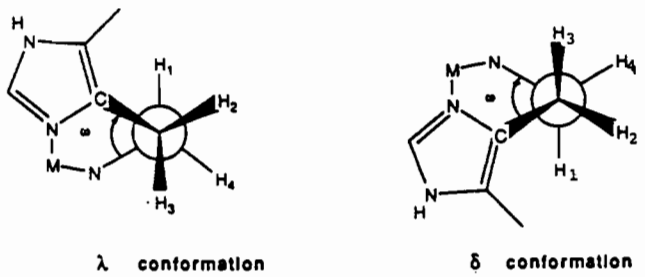

Figure 4. Newman projections of the six-member chelate rings in $[Zn^{II}((5\text{-MeimidH})_2DAP)]^{2+}$: staggered λ and δ conformations ($\phi = \omega = 60°$).

Because the molecule is chiral, it exists in the crystal as the two symmetry-related enantiomers. Figure 3 shows the Δ(λ,λ) isomer, whereas its enantiomer is Λ(δ,δ). Here Λ and Δ are used to describe the absolute configuration of these dissymmetric complexes when the dissymmetry is due to the chelate ring (arm) distribution about the metal (i.e., the molecular configuration). Δ is used when the rings describe a right-handed helix as the complex is viewed along the C_2 axis, and Λ is used when they describe a left-handed helix. In addition, δ and λ are used to describe the conformations of the individual six-membered chelate rings. Thus, δ denotes a ring of right-handed helicity and λ denotes a ring of left-handed helicity, as illustrated in Figure 4. This nomenclature parallels that of the IUPAC convention for tris(bidentate) complexes.[21]

NMR Spectra. Complete ^1H NMR spectra of the three Zn(II) cations in CD_3CN at 293 K are given in Figure 1. Proton resonance assignments and signal positions appear in the Experimental Section. As reported in a previous study, the spectra are consistent with the formulation of these complexes as five-coordinate species in solution.[14] For example, no additional multiplicity of the kind possible for uncoordinated ligand arms is apparent. The methylene portion of the spectrum does not exhibit the same

(21) *Inorg. Chem.* **1970**, 9, 1–5.

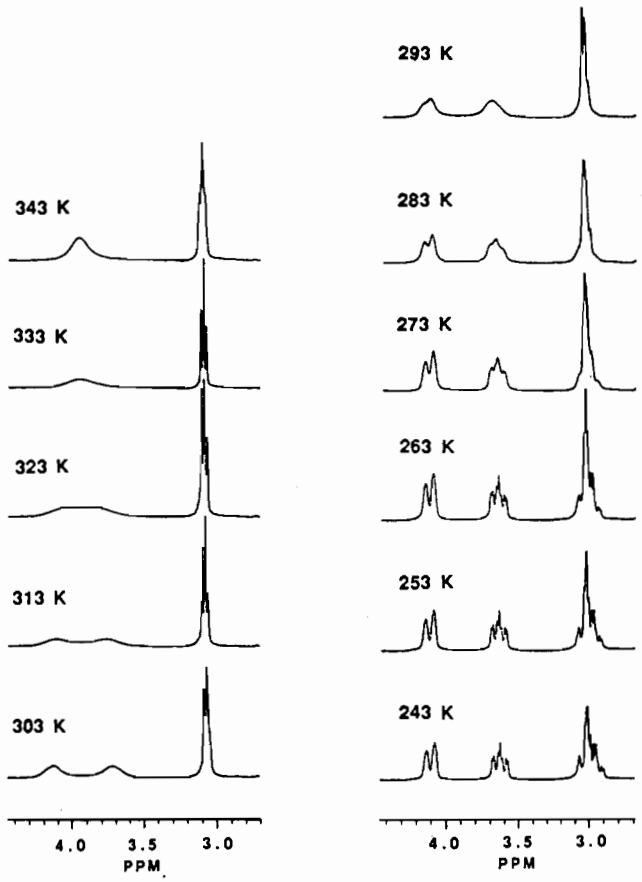

Figure 5. 300-MHz variable-temperature ^{1}H NMR spectra of the methylene proton region for $[Zn^{II}((5\text{-MeimidH})_2DAP)]^{2+}$ in CD_3CN.

number of signals for all three compounds. Both $[Zn^{II}((5\text{-MeimidH})_2DAP)]^{2+}$ and $[Zn^{II}((imidH)_2DAP)]^{2+}$ have three multiplets with relative peak areas of 1:1:2, with the spectrum of the former showing greater resolution; $[Zn^{II}((py)_2DAP)]^{2+}$ displays only two multiplets with relative peak areas of 1:1. The significance of these differences will become evident when the temperature dependence is taken into consideration. Note also that the spectrum of $[Zn^{II}((imidH)_2DAP)]^{2+}$ differs significantly from that reported previously,[14] where two methylene multiplets were observed with relative peak areas of 1:1; the difference is attributed to the lower field of the prior study (90 MHz).

Figure 5 shows the variable-temperature ^{1}H NMR spectrum of the methylene proton region for $[Zn^{II}((5\text{-MeimidH})_2DAP)]^{2+}$ in CD_3CN. At the highest temperature (343 K) the spectrum is similar to that of $[Zn^{II}((py)_2DAP)]^{2+}$ at 293 K (Figure 1) in that there are two signals with relative peak areas of 1:1. Because the molecule is chiral and because the X-ray crystal structure shows that the two arms of the ligand are interchangable by rotation about a C_2 axis, a total of four nonequivalent methylene protons should exist in the molecule, assuming the molecular structure is not altered in solution. Apparently at the higher temperatures (333 K and above), not only are the two ligand arms equivalent but also the two protons of each methylene group are also equivalent. This indicates that the molecule undergoes a dynamic exchange process that leads to averaging within the geminal sites. As the temperature is lowered, the downfield signal gradually broadens and eventually separates into two peaks. The chemical shifts of these two peaks change as a function of temperature until the spectrum at 253 K is obtained. By this temperature, three highly resolved multiplets with relative peak areas of 1:1:2 are obtained. The sharper upfield signal in the 343 K spectrum does not exhibit the same dramatic temperature dependent behavior of the downfield signal. Instead, it appears as a single signal, displaying relatively small changes as the temperature is lowered. Other portions of the NMR spectrum show only a slight narrowing of the signals as the temperature is lowered, and the 2,2′ proton resonance changes from a singlet to a narrow doublet separated by 1.4 Hz. At 243 K, the observed splitting pattern in the methylene region is interpreted as being due to two pairs of multiplets arising from four nonequivalent methylene protons in which the high-field pair of multiplets overlaps. Coalescence occurs at 328 ± 5 K for the low-field pair, and peak separation of the finally resolved resonances is approximately 140 Hz (see the 243 K spectrum).

Table V. Summary of the Coalescence Data for the Zn(II) and Cu(II) Complexes from the Variable-Temperature ^{1}H NMR Kinetics Experiments

complex	T_c, K	τ_c, ms	k_c, s^{-1}	$\Delta G_c^{\ddagger}$, kJ mol^{-1}	solvent
$[Zn^{II}((5\text{-MeimidH})_2DAP)]^{2+}$	328 (±5)	1.6	313	65	*b*
	≫298	1.4	357		*c*
$[Zn^{II}((imidH)_2DAP)]^{2+}$	308 (±5)	1.45	345	61	*b*
	288 (±5)	1.3	385	56	*c*
$[Zn^{II}((py)_2DAP)]^{2+}$	273 (±10)				*b*
	268 (±5)	1.6	313	53	*c*
$[Cu^{I}((py)_2DAP)]^{\bullet}$	253 (±10)	1.65	303[a]	50	*d*
	...[e]		...	...	*b*
$[Cu^{I}((imidH)_2DAP)]^{+}$	...[e]		...	...	*d*
	≪243[f]				*b*
$[Cu^{I}((5\text{-MeimidH})_2DAP)]^{+}$	203 (±10)				*d*
	≪243[f]				*b*

[a] The value of 400 s^{-1} previously reported was due to a typographical error.[6] [b] In CD_3CN. [c] In acetone-d_6. [d] In CD_2Cl_2. [e] No variable-temperature measurements in the specified solvent. [f] Exchange-averaged spectra were observed at all temperatures.

In the methylene proton region, the ^{1}H NMR spectra of both $[Zn^{II}((imidH)_2DAP)]^{2+}$ and $[Zn^{II}((py)_2DAP)]^{2+}$ exhibit temperature dependences qualitatively similar to that of $[Zn^{II}((5\text{-MeimidH})_2DAP)]^{2+}$; however, coalescence occurs at different temperatures. A spectrum without exchange broadening is never observed for $[Zn^{II}((py)_2DAP)]^{2+}$, even at the lowest temperatures attained, and it is unclear as to whether one is actually observed for $[Zn^{II}((imidH)_2DAP)]^{2+}$. Other portions of the spectrum for both compounds show a slight narrowing of the signals as the temperature is lowered. Only the 2,2′-proton resonance of $[Zn^{II}((imidH)_2DAP)]^{2+}$ changes multiplicity with temperature, converting from a singlet to a narrowly spaced doublet (0.90 Hz) in CD_3CN by 283 K. Complete variable-temperature ^{1}H NMR chemical shift data at 300 MHz for the three Zn(II) complexes in CD_3CN and acetone-d_6 are available in the supplementary material. Coalescence temperatures, T_c, are presented in Table V.

As reported previously for $[Cu^{I}((py)_2DAP)](BF_4)$ in CD_2Cl_2,[6] variable-temperature studies of the analogous Cu(I) compounds indicate that these molecules also undergo a dynamic exchange process. $[Cu^{I}((imidH)_2DAP)](BF_4)$ could not be studied in CD_2Cl_2 because it is not soluble, but $[Cu^{I}((5\text{-MeimidH})_2DAP)](BF_4)$ is very soluble. In CD_2Cl_2, the two methylene proton resonances of this compound remain sharp as the temperature is lowered to 233 K (Figure 6), but by 213 K, significant broadening is observed. When the temperature is lowered to 203 K, the signals broaden to such a degree they are barely discernible, and by 193 K, four very broad signals appear to be observed. Thus, coalescence for this compound is around 203 K. Other portions of the spectrum show a slight narrowing of the peaks as the temperature is lowered, with the one exception that the methyl 5,5′-proton resonance displays significant broadening at 243 K and continues to broaden as the temperature is lowered.

In CD_3CN at room temperature, all three of the Cu(I) compounds display two peaks in the methylene proton region with relative peak areas of 1:1, as exemplified by the spectrum of $[Cu^{I}((5\text{-MeimidH})_2DAP)]^{+}$ in Figure 2. Variable-temperature experiments in this solvent have been performed for $[Cu^{I}((5\text{-MeimidH})_2DAP)]^{+}$ and $[Cu^{I}((imidH)_2DAP)]^{+}$. For both of the compounds, the methylene proton resonances sharpen and narrow as the temperature is lowered to 243 K, the lowest temperature achievable in this solvent. There is no broadening of the signals, and there is no change in the number of resonances. Other portions of the spectrum show the same narrowing of the signals

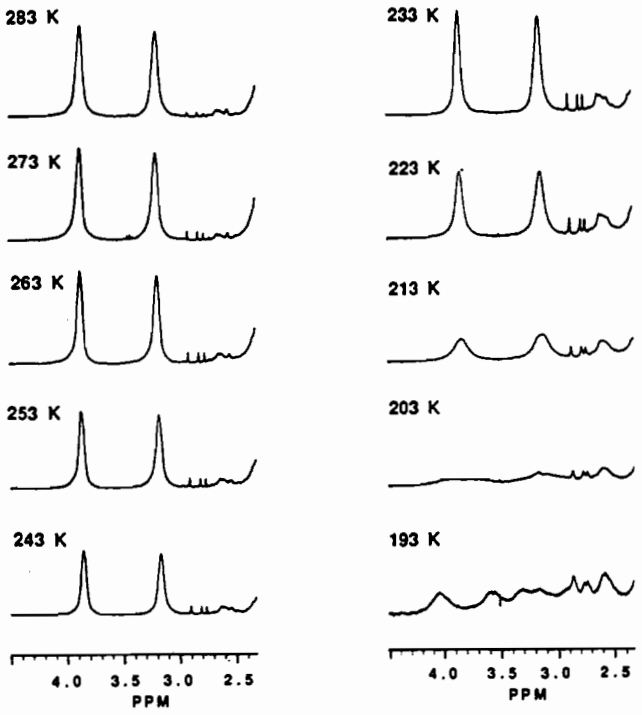

Figure 6. 300-MHz variable-temperature ^{1}H NMR spectra of the methylene proton region for $[Cu^I((5\text{-MeimidH})_2DAP)]^+$ in CD_2Cl_2.

Table VI. Resonance Frequencies ν (Hz), Line Broadening LB (Hz), and Coupling Constants $J_{i,j}$ (Hz) for the Calculated Spectra of $[Zn^{II}((5\text{-MeimidH})_2DAP)]^{2+}$ and $[Cu^I((py)_2DAP)]^+$

T, K	$\nu(1)$	$\nu(2)$	$\nu(3)$	$\nu(4)$	LB
		$[Zn^{II}((5\text{-MeimidH})_2DAP)]^{2+}$			
243	1092.900	914.750	891.250	1232.250	3.5
$J_{1,2}$ = 3.6	$J_{1,3}$ = 12.5	$J_{1,4}$ = −16.0	$J_{2,3}$ = −16.0	$J_{2,4}$ = 2.0	$J_{3,4}$ = 4.8
		$[Cu^I((py)_2DAP)]^+$			
193	1147.681	959.435	1140.663	1282.228	7.5
$J_{1,2}$ = 3.4	$J_{1,3}$ = 13.7	$J_{1,4}$ = −14.0	$J_{2,3}$ = −14.0	$J_{2,4}$ = 2.3	$J_{3,4}$ = 4.6

as the temperature is lowered. Complete variable-temperature ^{1}H NMR chemical shift data for $[Cu^I((5\text{-MeimidH})_2DAP)]^+$ in CD_2Cl_2 and CD_3CN and for $[Cu^I((imidH)_2DAP)]^+$ in CD_3CN are available in the supplementary material. Attempts to obtain lower temperature spectra by use of CH_2Cl_2/CH_2F_2 solvent mixtures failed because of the limited solubility of the Cu(I) complexes. Coalescence data for the Cu(I) complexes are summarized in Table V.

Spectral Simulation. Figure 7 presents the results of a spectral simulation study of the methylene proton region for $[Zn^{II}((5\text{-MeimidH})_2DAP)]^{2+}$ in CD_3CN at 243 K. Plot A is the experimentally observed spectrum, while plot B is the simulated spectrum. Resonance frequencies and coupling constants are listed in Table VI. The calculated spectrum is in good agreement with the observed experimental spectrum. The pattern is that of an ABMX system arising from four chemical shift nonequivalent methylene protons. As discussed below, the methylene proton coupling constants listed in Table VI are consistent with a nearly fully staggered conformation about the methylene C–C bond. Assignments for the spectrum at 243 K have been made by assuming a conformation similar to that found in the crystal structure and using the Karplus relationship of vicinal proton coupling constants to the dihedral angle (ϕ) between the H–C–C′ and the C–C′–H′ planes.[22]

From the temperature dependence, it is clear that resonances 1 and 4 and resonances 2 and 3 in Table VI correspond to geminal pairs. This is consistent with a value of −16 Hz for $J_{1,4}$ and $J_{2,3}$ as is generally observed for geminal pairs.[22] Second, it is generally

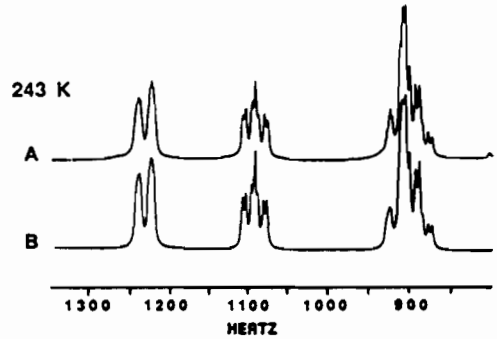

Figure 7. 300-MHz low-temperature ^{1}H NMR spectra of the methylene proton region for $[Zn^{II}((5\text{-MeimidH})_2DAP)]^{2+}$ in CD_3CN: (A) experimental spectrum; (B) calculated spectrum.

observed that vicinal couplings are largest between protons related by a dihedral angle, ϕ, of nearly 0 or 180° and smallest for a dihedral angle of nearly 90°.[22] Consequently, the coupling constant of $J_{1,3}$ = 12.5 Hz is assigned to the trans-axial axial protons. Thus the assignment of the protons as in Figure 4 is consistent with the resonances in Table VI. From the Karplus relationship, a coupling constant for $J_{1,3}$ of 12.5 Hz implies $\phi \approx 60°$ and a chelate ring in a nearly fully staggered configuration for $[Zn^{II}((5\text{-MeimidH})_2DAP)]^{2+}$ as shown in Figure 4.

Chemical shift nonequivalence between the α,α'- and β,β'-methylene groups is easily understood since their chemical environments are quite different, with the α,α' group adjacent to an imine nitrogen atom and a methylene carbon atom and the β,β' group adjacent to a methylene carbon atom and an imidazole ring carbon atom. Chemical shift nonequivalence between the geminal protons may be due to their proximity to the chiral metal center, to the differential shielding of axial vs equatorial protons, and to the presence of ring currents in the imidazole moieties. In the case of the β,β'-protons, these effects nearly cancel, and because the chemical shift difference between the two ($\Delta\nu_{2,3}$ = 20 Hz) is of the same magnitude as the geminal coupling constant ($J_{2,3}$ = −16 Hz), their resonances give rise to the AB portion of the spectrum.

The experimental spectrum of $[Cu^I((py)_2DAP)]^+$ in CD_2Cl_2 has been reported previously.[6] At low temperatures, the pattern is that of an ABMX system arising from four chemical shift nonequivalent methylene protons. As for the Zn(II) case, the temperature dependence shows that resonances 1 and 4 and resonances 2 and 3 must reflect geminal pairs. The simulated spectrum was generated with the aid of PCMODEL.[23] This molecular mechanics program was used to generate an energy-minimized structure similar to that shown in the crystal structure; the program then gave the four vicinal coupling constants according to the empirical relationship of Haasnoot et al.[24] Geminal coupling constants of −14 Hz were selected by analogy with similar systems. Resonance frequencies were derived by inspection of the experimental spectrum. Excellent agreement between the low-temperature spectrum and the simulated spectrum (in the supplementary material) was obtained by using the resonance frequencies and coupling constants listed in Table VI. The simulations were performed by using these coupling constants and chemical shifts. Simulations with PANIC showed that the large trans-axial–axial coupling constant had to be assigned to $J_{1,3}$. This required assignment of the equatorial–equatorial coupling constant of 2.29 Hz to $J_{2,4}$. Assignments of $J_{1,2}$ as 3.37 Hz and $J_{3,4}$ as 4.56 Hz or vice versa did not lead to significant differences; the former assignment is preferred because it places protons 1 and 4 in the α-position, which is the relationship to be expected on the basis of inductive effects on chemical shifts. Thus the assignment as presented is consistent with the numbering scheme in Figure 4,

(22) Bovey, F. A. *Nuclear Magnetic Resonance Spectroscopy*, 2nd ed.; Academic Press: San Diego, CA, 1988; pp 118–119, 191–203.

(23) PCMODEL: Molecular Modeling Software for the Macintosh II. Serena Software: Bloomington, IN. This is a molecular mechanics program based on MMX, an enhanced version of MM2.

(24) Haasnoot, C. A. G.; de Leeuw, F. A. A. M.; Altona, C. *Tetrahedron* **1980**, *36*, 2783–2792.

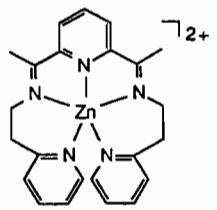

$[Zn^{II}((py)_2DAP)]^{2+}$

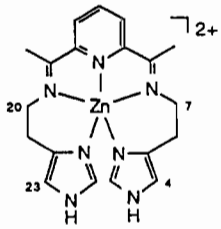

$[Zn^{II}((imidH)_2DAP)]^{2+}$

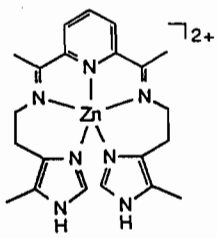

$[Zn^{II}((5\text{-}MeimidH)_2DAP)]^{2+}$

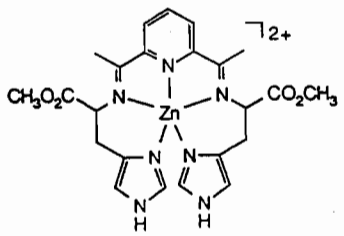

$[Zn^{II}((L\text{-}bisp)]^{2+}$

Figure 8. Schematic representations of the pentacoordinate zinc cations: $[Zn^{II}((py)_2DAP)]^{2+}$, $[Zn^{II}((imidH)_2DAP)]^{2+}$; $[Zn^{II}((5\text{-}MeimidH)_2DAP)]^{2+}$; $[Zn^{II}(L\text{-}bisp)]^{2+}$.

and the simulated spectrum at 193 K is in good agreement with the experimental spectrum. Chemical shift nonequivalence between the α,α'- and β,β'-methylene groups occurs for the same reasons discussed above for $[Zn^{II}((5\text{-}MeimidH)_2DAP)]^{2+}$, and once again, the nonequivalence of the geminal protons is probably due to the adjacent chiral Cu(I) metal center, axial vs equatorial shielding, and ring currents. In this case these effects lead to the β-equatorial proton having a resonance upfield from the β-axial proton, which is contrary to the rule for simple aliphatic systems.[22] Ratios of chemical shift differences to coupling constants, $\Delta\nu_{ij}/J_{ij}$, show that each pair of geminal protons are weakly coupled. All of the vicinal coupling interactions are also weak except for one, in that the chemical shift difference between H_1 and H_3 ($\Delta\nu_{1,3}$ = 7.0 Hz) is of the same magnitude as their coupling constant ($J_{1,3}$ = 13.7 Hz). Thus, the AB portion of the spectrum is due to some overlap of these resonances. Similar analyses for $[Cu^{I}((imidH)_2DAP)]^{+}$ and $[Cu^{I}((5\text{-}MeimidH)_2DAP)]^{+}$ could not be performed because spectra without exchange broadening were never realized, even at the lowest obtainable temperatures.

Discussion

Solid-State Structure. Crystal structures of two, related pentacoordinate Zn(II) cations, $[Zn^{II}((imidH)_2DAP)]^{2+}$ [25] and $[Zn^{II}(L\text{-}bisp)]^{2+}$ (Figure 8),[26] have been previously reported. Both $[Zn^{II}((5\text{-}MeimidH)_2DAP)]^{2+}$ and $[Zn^{II}(L\text{-}bisp)]^{2+}$ can be considered derivatives of $[Zn^{II}((imidH)_2DAP)]^{2+}$, as shown in the figure. Substitution of a methyl group for the proton on carbons C(4) and C(23) gives $[Zn^{II}((5\text{-}MeimidH)_2DAP)]^{2+}$, while substitution of a methyl ester group for a proton on carbons C(7) and C(20) gives $[Zn^{II}(L\text{-}bisp)]^{2+}$. All of these structures share the general feature of having a pentadentate ligand enveloping the metal ion in the same fashion. However, the details of the inner coordination spheres and ligand conformations differ somewhat for the three compounds.

As in $[Zn^{II}((imidH)_2DAP)](ClO_4)_2$ and $[Zn^{II}(L\text{-}bisp)](ClO_4)_2$, the metal atom in $[Zn^{II}((5\text{-}MeimidH)_2DAP)](BF_4)_2$ is bonded to five nitrogen atoms and displays a coordination geometry herein described as a distorted trigonal bipyramid. The Zn–N bond distances are listed in Table VII, and some selected bond angles

Table VII. Comparison of Zn–N Bond Distances (Å) in the $[Zn^{II}((5\text{-}MeimidH)_2DAP)]^{2+}$, $[Zn^{II}((imidH)_2DAP)]^{2+}$, and $[Zn^{II}(L\text{-}bisp)]^{2+}$ Structures

nitrogen atom	$[Zn^{II}((5\text{-}MeimidH)_2DAP)]^{2+}$ [a]	$[Zn^{II}((imidH)_2DAP)]^{2+}$ [b]	$[Zn^{II}(L\text{-}bisp)]^{2+}$ [c]
central pyridine	2.04 (1)	2.067 (5)	2.032 (2)
terminal rings	1.99 (1)	1.988 (5)	1.996 (3)
	2.01 (1)	1.992 (5)	1.998 (3)
imine	2.18 (1)	2.180 (5)	2.194 (2)
	2.171 (7)	2.171 (5)	2.196 (3)
av tot.[d]	2.08	2.08	2.08
av plane[e]	2.02	2.02	2.01
av axial[f]	2.18	2.18	2.19

[a] This work. [b] From reference 25. [c] From reference 26. [d] Average of five values. [e] Average of three values. [f] Average of two values.

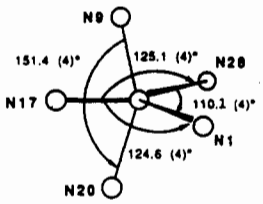

$[Zn^{II}((5\text{-}MeimidH)_2DAP)]^{2+}$

L-s Plane	Dihedral Angle
1 - 2	112.35°
1 - 3	76.28°
2 - 3	69.47°

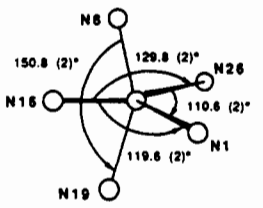

$[Zn^{II}((imidH)_2DAP)]^{2+}$

L-s Plane	Dihedral Angle
1 - 2	72.3°
1 - 3	106.1°
2 - 3	59.3°

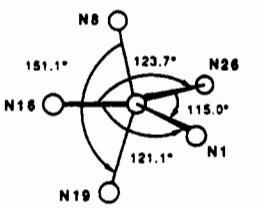

$[Zn^{II}(L\text{-}bisp)]^{2+}$

From reference 26

Figure 9. Bond angles within the inner coordination sphere of the pentacoordinate Zn(II) cations with dihedral angles between least-squares planes for two of the cations.

are depicted in Figure 9. The average bond distance to the three trigonal atoms is 2.02 (1), 2.016 (5), and 2.009 (3) Å for $[Zn^{II}((5\text{-}MeimidH)_2DAP)]^{2+}$, $[Zn^{II}((imidH)_2DAP)]^{2+}$, and $[Zn^{II}(L\text{-}bisp)]^{2+}$, respectively, whereas the average distance to the "axial" imine atoms is 2.18 (1), 2.175 (5), and 2.195 (3) Å. These longer axial interactions are important to the present interpretation of the coordination geometry, since they define the unique axis. Previous interpretations have described the geometry about the metal as intermediate between a trigonal bipyramid and a square pyramid, rather than as a quasi-trigonal-bipyramidal structure.[25,26] The latter interpretation is favored when the Zn–N bond distances are considered in conjunction with the bond angles around zinc.

Another similarity the compounds share is in their conformations. With the exception of $[Zn^{II}(L\text{-}bisp)]^{2+}$, all the complexes crystallize as racemic mixtures of the enantiomeric $\Delta(\lambda,\lambda)$ and $\Lambda(\delta,\delta)$ isomers. This is true for both $[Zn^{II}((imidH)_2DAP)](ClO_4)_2$[25] and $[Zn^{II}((5\text{-}MeimidH)_2DAP)](BF_4)_2$, and similar results have been observed for $[Cu^{I/II}((py)_2DAP)]^{n+}$,[4] $[Cu^{I/II}((imidH)_2DAP)]^{n+}$,[25] and $[Cu^{II}((5\text{-}MeimidH)_2DAP)]^{2+}$.[8] Because L-bisp is inherently chiral, $[Zn^{II}(L\text{-}bisp)]^{2+}$ crystallizes as the optically active $\Delta(\lambda,\lambda)$ isomer.[26] In principle, the isomers $\Delta(\lambda,\delta)$, $\Delta(\delta,\delta)$, $\Lambda(\lambda,\lambda)$, and $\Lambda(\lambda,\delta)$ could exist, as shown by molecular models. Such species, however, have not been found in any of the crystal structures.

(25) Korp, J. D.; Bernal, I.; Merrill, C. L.; Wilson, L. J. *J. Chem. Soc., Dalton Trans.* **1981**, 1951–1956.
(26) Casella, L.; Silver, M. E.; Ibers, J. A. *Inorg. Chem.* **1984**, *23*, 1409–1418.

Table VIII. Comparison of Cu–N Bond Distances (Å) in the $[Cu^{I}((py)_2DAP)]^+$, and $[Cu^{I}(imidH)_2DAP)]^+$ Structures

nitrogen atom	$[Cu^{I}((py)_2DAP)]^{+a}$	$[Cu^{I}((imidH)_2DAP)]^{+b}$
central pyridine	2.094 (14)	1.895 (33)
terminal rings	2.032 (12)	1.887 (29)
	2.083 (12)	1.933 (31)
imine	2.273 (14)	2.282 (31)
	2.240 (14)	2.534 (29)
av tot.[c]	2.14	2.11
av plane[d]	2.07	1.91
av axial[e]	2.26	2.41

[a] From reference 4. [b] From reference 5. [c] Average of five values. [d] Average of three values. [e] Average of two values.

Detailed differences in the inner coordination sphere are more apparent when comparing bond angles instead of bond distances. The angles from the central pyridine nitrogen to the two imidazole nitrogens are most alike in $[Zn^{II}((5\text{-MeimidH})_2DAP)]^{2+}$, with a difference of only 0.5° compared to 2.6° and 10.2° for $[Zn^{II}$-(L-bisp)$]^{2+}$ [26] and $[Zn^{II}((imidH)_2DAP)]^{2+}$,[25] respectively. A comparison of the dihedral angles between equivalent least-squares planes (Figure 9) for $[Zn^{II}((5\text{-MeimidH})_2DAP)]^{2+}$ and its parent complex shows that there are significant differences in the detailed molecular structure of these complexes. The overall features of the $((5\text{-MeimidH})_2DAP)$ coordination group are closer to the idealized C_2 symmetry than is found for the $((imidH)_2DAP)$ compound. In the present case, an idealized C_2 axis bisects the pyridine ring and includes the Zn–N(17) bond. The idealized C_2 symmetry of $[Zn^{II}((5\text{-MeimidH})_2DAP)]^{2+}$ is the maximum symmetry that this chiral compound, and its related analogues, can possess. Despite these differences in the molecular structure, both $[Zn^{II}((imidH)_2DAP)]^{2+}$ and $[Zn^{II}((5\text{-MeimidH})_2DAP)]^{2+}$ crystallize in the centrosymmetric space group $C2/c$ with $Z = 8$.[25] However, since the two crystal packing diagrams are qualitatively different, it is still possible that the differences in molecular structure are due to crystal packing forces.

Structures in Solution. Simulations of the ^1H NMR spectra have shown that the spectra are entirely consistent with the molecules in solution having the same conformations as found in the crystal structures. On the other hand, inspection of molecular models shows that various other conformations of the complexes in principle can exist. For example, a simple conformational twist of one of the dimethylene units can convert the $\Delta(\lambda,\lambda)$ form to the asymmetric $\Delta(\delta,\lambda)$ form. Thus, in addition to the enantiomeric pair $\Delta(\lambda,\lambda)$, $\Lambda(\delta,\delta)$ seen in the crystal structures, two other pairs can be envisaged: $\Delta(\lambda,\delta)$, $\Lambda(\delta,\lambda)$ and $\Delta(\delta,\delta)$, $\Lambda(\lambda,\lambda)$. It is of some concern as to whether these conformers are significant species in solution. Simulations with PANIC have shown that the observed ^1H NMR spectra can indeed be generated by these other conformers with reasonable values for the chemical shifts and coupling constants. Clearly the problem is whether the solutions consist of the crystal conformers exclusively or they have a mixture of various conformers.

The low-temperature NMR spectra require that the various conformers, if present in solution, have nearly identical spectra. This seems quite unlikely, in view of the significant differences in metal shielding and ring currents to be expected for the various conformers. Moreover, to have a mixture of conformers requires that they have similar energies. We have investigated the problem of energetics by conducting strain energy calculations with PCMODEL. The application of molecular mechanics to coordination complexes has recently been reviewed.[27] For the case of $[Cu^{I}$-$((py)_2DAP)]^+$, the $\Delta(\lambda,\lambda)$ conformer is predicted to have 4.6 kcal less strain energy than the asymmetric $\Delta(\lambda,\delta)$ conformer, with the $\Delta(\delta,\delta)$ conformer yet higher in energy. Thus the lowest energy conformer calculated by PCMODEL is also the conformer seen in the crystal structure. A difference of 4.6 kcal would make the population of the higher energy conformer contribute insignificantly to the NMR spectrum. Since it is unlikely that both conformers will have the same spectra as well as be isoenergetic, we believe that the solutions are composed primarily of the enantiomeric pairs of conformations seen in the crystal structures.

Mechanism of Exchange. A characteristic feature of the ^1H NMR spectra is the temperature dependence of the methylene regions for the Zn(II) as well as the Cu(I) complexes. The temperature dependence requires a dynamic exchange process that leads to equivalence of the four α- and the four β-protons. The same effect was previously observed for the $[Cu^{I}((py)_2DAP)]^+$ complex.[6]

There are several possible mechanisms for the dynamic exchange process seen in the NMR spectra. One pathway, designated as the twist mechanism, would involve simple rotation of the protons about the methylene C–C bond in the chelate ring. Protons originally in an axial position would be rotated into an equatorial position and vice versa, and the compound would remain pentacoordinate throughout the inversion process. This would entail conversion between the $\Delta(\lambda,\lambda)$ and $\Delta(\delta,\lambda)$ conformers. If the two conformers had essentially identical low-temperature spectra, the spectrum of the α-protons at the high-temperature limit would appear as a pair of peaks, separated by the population-weighted difference of the low-temperature chemical shifts. In order to lead to the observed single peaks at high temperatures, this mechanism would require that the two conformers differ in energy by less than 1 kcal/mol and that the two have essentially identical spectra. For the reasons mentioned above, this is viewed as highly unlikely.

The second and third pathways, designated as bond-rupture mechanisms, involve partial ligand dissociation and reattachment of the ligand arms, proceeding through different, four-coordinate intermediates. One intermediate could result from the breaking of one of the metal-to-arm terminal nitrogen bonds, while a second possible intermediate could occur by breaking a M–N(imine) nitrogen bond. Both of these bond-rupture mechanisms require intermediates that destroy the C_2 symmetry of the molecule. Therefore, the presence of a four-coordinate species in any appreciable concentration (5–10%) would result in a more complex NMR spectrum than is observed. Because the above variable-temperature spectra can be successfully analyzed by assuming only five-coordinate species of C_2 symmetry, the present data require that such four-coordinate intermediates be present in quite low concentration. However, our previous ligand substitution kinetics study of $[Cu^{I}((py)_2DAP)]^+$ by $[Zn^{II}(CH_3CN)_6]^{2+}$ indicates that a bond-rupture mechanism is a facile process (k_d was determined to be 310 s^{-1}).[6] If the outcome of the bond rupture is formation of the opposite conformer for a single six-membered ring, then the mechanism can be discarded for the same reasons as was the twist mechanism. On the other hand, it is conceivable that bond rupture is followed by optical inversion at the metal center, leading to interconversion between the $\Delta(\lambda,\lambda)$ and $\Lambda(\delta,\delta)$ enantiomers. These species, by definition, have identical ^1H NMR spectra, and are isoenergetic. Furthermore, the optical inversion leads to exchange of the equatorial and axial protons. The possibility of optical inversion for a non-bond-rupture mechanism is unlikely because the transition state would have a sterically unfavorable "planar" geometry. By inspection of molecular models, it is difficult to see how rupture of the M–N(imine) bond could lead to optical inversion. Thus we are left with the most likely exchange mechanism being M–N(terminal) bond rupture followed by optical inversion.

Rates of Exchange. A chemical exchange process is considered to be slow, on the NMR time scale, when the resonances of the exchanging nuclei are observed separately without broadening. Under conditions of fast exchange, the signals of the exchanging nuclei have merged into a single peak and the observed chemical shift is a weighted average of the two resonances.[28–30] Line-shapes are correctly predicted, for systems that are not spin–spin coupled,

(27) Hancock, R. D. *Prog. Inorg. Chem.* **1989**, *37*, 187–291.

(28) Drago, R. S. *Physical Methods in Chemistry*; W. B. Saunders: Philadelphia, PA, 1977; pp 252–257.

(29) Martin, M. L.; Delpuech, J.-J.; Martin, G. J. *Practical NMR Spectroscopy*; Heyden: London, 1980; pp 291–311.

(30) Pople, J. A.; Schneider, W. G.; Bernstein, H. J. *High-resolution Nuclear Magnetic Resonance*; McGraw-Hill: New York, 1959; pp 218–230.

by introducing the influence of chemical exchange into the Bloch equations.[28-30] This classical approach is also applicable to line-shape calculations for exchanging multiplets provided the coupling constants are much smaller than the differences in the chemical shift frequencies.[29] When dealing with strongly coupled spin systems, it becomes necessary to use the quantum-mechanical treatment adopted by density matrix theory.[28,29] Since portions of the spectra in this paper are strongly coupled, a rigorous treatment would entail a complete line-shape analysis.

However, there are limiting cases that can be utilized to obtain the lifetimes, τ, without having to resort to a total line-shape simulation.[28,29] In the absence of exchange, the two environments, A and B, appear as two distinct signals centered at frequencies ν_A and ν_B, respectively. As the exchange rate increases from zero to the fast exchange limit, there is a broadening of the signals centered at ν_A and ν_B followed by overlap and then coalescence into a single, broad, flat-topped peak that narrows into the single, sharp line of the fast-exchange limit. At coalescence $(\nu_A - \nu_B)_{obs}$ is equal to zero, and the lifetime at coalescence, τ_c, can be obtained from eq 1.[30] In this equation $(\nu_{A_0} - \nu_{B_0})$ is the separation of peaks

$$\tau_c = 2^{1/2}/2\pi(\nu_{A_0} - \nu_{B_0}) \quad (1)$$

in the absence of exchange broadening in Hz. Equation 1 is valid under the following conditions: (a) no coupling between resonances A and B; (b) equal populations and lifetimes so that $N_A = N_B = {}^1/_2$ and $\tau_A = \tau_B = 2\tau$; (c) long intrinsic transverse relaxation times so that $1/T_{2A} = 1/T_{2B} = 0$. The low-temperature spectra of these pentacoordinate compounds clearly show that the methylene protons are spin–spin coupled. For certain of the peaks the coupling is weak enough that condition a is closely approximated. Condition b is strictly fulfilled, because the exchange mechanism is optical inversion. Condition c simply requires that the signal widths in the absence of exchange be small relative to their separation, and in the present cases it is fulfilled by those signals that meet condition a.

Because the chemical environment of the α,α'-methylene group is different from that of the β,β' group, the spin system has been considered as two separate, two-site exchange centers. In the Zn(II) compounds, the β,β' resonances display a second-order spectrum, since the chemical shift difference of H_2 and H_3 ($\Delta\nu_{2,3}$ = 20 Hz) is of the same magnitude as the geminal coupling constant ($J_{2,3}$ = −16 Hz). Therefore, it is not possible with eq 1 to obtain information concerning the exchange rates from these signals. Rate data can, however, be obtained from consideration of the α,α' resonances. A peak separation $(\Delta\nu_{A_0,\nu_{B_0}})$ of 140 Hz is observed for $[Zn^{II}((5\text{-MeimidH})_2DAP)]^{2+}$ in CD_3CN at 243 K. From eq 1, this separation leads to a lifetime, τ_c, of 1.6 ms at coalescence, 328 ± 5 K. Because the coupling constants are generally less than 20 Hz in this and the other systems, the uncertainty in τ_c due to coupling is believed to be less than 20%. Variable-temperature measurements in acetone-d_6, like those in CD_3CN, appear to be in the nonexchanging region at the lower temperatures (213 K and below). The observed peak separation of 165 Hz corresponds to a lifetime of a 1.4 ms at coalescence, although only a lower limit is known for the coalescence temperature. Because spectra without exchange broadening are not observed for the other Zn(II) compounds, values for $(\Delta\nu_{A_0,\nu_{B_0}})$ can not be determined. However, if the peak separations at the lowest temperatures are assumed to be near the low-temperature limit, an upper-limit lifetime can be calculated. In the case of $[Zn^{II}((imidH)_2DAP)]^{2+}$, this assumption has been made for the data in both solvents. The peak separation in CD_3CN at 243 K is 155 Hz for a lifetime of 1.45 ms at 308 ±5 K. In acetone-d_6, the peak separation at 213 K is 173 Hz, which corresponds to a lifetime of 1.3 ms at 288 ± 5 K. For $[Zn^{II}((py)_2DAP)]^{2+}$, the low-temperature data are almost full of exchange broadening in acetone-d_6 but not CD_3CN. A peak separation of 141 Hz at 213 K leads to a lifetime of 1.6 ms at 268 ± 5 K. For $[Cu^{I}((py)_2DAP)]^{+}$ in CD_2Cl_2, both the α,α' and β,β' protons displayed first-order spectra at low temperature, and coalescence was observed for both sets of protons; the low-temperature peak separations were reported as 110 and 180 Hz with corresponding lifetimes of 2.1 and 1.3 ms at coalescence, 253 ± 10 K.[6] It was presumed that these lifetimes pertained to the same rate process and reflected slightly different coalescence temperatures. Because coalescence for $[Cu^{I}((5\text{-MeimidH})_2DAP)]^{+}$ is at 203 ± 10 K and the lowest obtainable temperature was 193 K, a lifetime could not be ascertained. The coalescence temperatures and lifetimes for the Zn(II) and Cu(I) compounds are summarized in Table V.

A comparison of the coalescence temperatures, T_c, in Table V orders the compounds according to their exchange rates: $[Zn^{II}((5\text{-MeimidH})_2DAP)]^{2+} < [Zn^{II}((imidH)_2DAP)]^{2+} < [Zn^{II}((py)_2DAP)]^{2+} < [Cu^{I}((py)_2DAP)]^{+} <$ $([Cu^{I}((imidH)_2DAP)]^{+}) < [Cu^{I}((5\text{-MeimidH})_2DAP)]^{+}$. Because $[Cu^{I}((imidH)_2DAP)]^{+}$ could not be studied in CD_2Cl_2 and $[Cu^{I}((py)_2DAP)]^{+}$ was not previously studied in CD_3CN,[6] it is difficult to determine the position in series for the former compound. However, the studies in CD_3CN demonstrate that the exchange rate is faster for $[Cu^{I}((imidH)_2DAP)]^{+}$ than for $[Zn^{II}((py)_2DAP)]^{2+}$, since an exchange-averaged spectrum is observed for this Cu(I) compound even at 243 K whereas coalescence occurs at (273 ± 10 K) for the most dynamic Zn(II) compound. To the degree that solvent effects can be ignored, the $[Cu^{I}((imidH)_2DAP)]^{+}$ complex can be ranked above $[Cu^{I}((py)_2DAP)]^{+}$ in the series.

Exchange rate constants at the coalescence temperatures can be derived from the lifetimes by

$$k_c = (2\tau_c)^{-1} \quad (2)$$

The factor of 2 appears because the rate constant refers to the "one-way" process.[31] Values of k_c are given in Table V. The free energy of activation, $\Delta G_c^{\ddagger}$, for the exchange process at the coalescence temperature, T_c, is related to τ_c by eq 3, where k, h, and R have their usual meaning. Values of $\Delta G_c^{\ddagger}$ so evaluated are also presented in Table V.

$$k_c = (kT/h)e^{-\Delta G_c^{\ddagger}/RT} \quad (3)$$

It is clear that the Cu(I) complexes undergo the exchange process considerably more readily than the Zn(II) complexes. Since the mechanism is believed to have M–N(terminal) bond breakage as the rate-limiting step, it is reasonable to expect the rates of exchange to show a trend similar to that for ligand substitution kinetics. The lesser charge at the Cu(I) center surely should lead to greater lability when comparing these d^{10} systems. We have no ready explanation for the fact that $[Cu^{I}((py)_2DAP)]^{+}$ exhibits the slowest exchange rate of the Cu(I) complexes, whereas its Zn(II) analogue is the fastest of the Zn(II) complexes.

One clarification to emerge in the present study relates to our prior study of the ligand-substitution kinetics of $[Cu^{I}((py)_2DAP)]^{+}$.[6] In that study the transfer of the ligand to $[Zn(CH_3CN)_6]^{2+}$ showed saturation kinetics, indicating rate-limiting breakage of the Cu–N(terminal) bond with a rate constant of 310 s^{-1} at 298 K. It was also reported (erroneously) that the rate of exchange of the axial and equatorial protons in that complex proceeded by the same rate-limiting step with a rate constant of 400 s^{-1} at 253 K. The present report resolves the discrepancy, by showing that the correct rate of exchange is only 303 s^{-1} at 253 K.

Another point of interest is that in the prior report it was found that the substitution reaction of $[Cu^{I}((imidH)_2DAP)]^{+}$ with $[Zn(CH_3CN)_6]^{2+}$ was much faster than that of $[Cu^{I}((py)_2DAP)]^{+}$. It is now clear that this effect is mirrored in the rates of methylene proton exchange. This lends further support to the concept that M–N(terminal) bond breakage is the rate-limiting step in the NMR line-broadening mechanism.

The present study considerably extends our understanding of the lability of pentacoordinate Zn(II) and Cu(I) complexes. By careful ligand design, it should be possible to systematically control and explore molecular dynamics in Cu(I) compounds, especially as it may relate to electron-transfer reactions involving the metal

(31) Reference 22, p 297.

center. The present and following papers represent our initial inquiry into this question.

Acknowledgment. At Rice University this work was supported by National Institutes of Health Grant GM-28451 from the National Institute of General Medical Sciences and Grant C-624 from the Robert A. Welch Foundation. The Rigaku AFC-5S X-ray diffractometer was purchased, in part, through an instrumentation grant from the National Science Foundation. Professor Mike Squillacote is thanked for helpful discussions regarding molecular mechanics and NMR spectroscopy.

Registry No. $[Zn^{II}((5\text{-MeimidH})_2DAP)](BF_4)_2$, 131702-91-5; $[Zn^{II}((imidH)_2DAP)](BF_4)_2$, 82135-49-7; $[Zn^{II}((py)_2DAP)](BF_4)_2$, 94629-92-2; $[Cu^{II}((5\text{-MeimidH})_2DAP)](BF_4)_2$, 131702-93-7; $[Cu^{I}((5\text{-MeimidH})_2DAP)](BF_4)$, 131726-89-1; $[Cu^{I}((imidH)_2DAP)](BF_4)$, 131726-90-4; $[Cu^{I}((py)_2DAP)](BF_4)$, 131702-94-8; 4-(carboethoxy)-5-methylimidazole, 51605-32-4; 5-methyl-4-(hydroxymethyl)imidazole hydrochloride, 38585-62-5; 5-methyl-4-(chloromethyl)imidazole hydrochloride, 51605-33-5; 5-methyl-4-(cyanomethyl)imidazole, 51667-66-4; 5-methylhistamine, 36507-31-0; 2,6-diacetylpyridine, 1129-30-2.

Supplementary Material Available: Tables S-II-S-V, listing anisotropic thermal parameters, hydrogen atom coordinates, rigid group parameters, and the calculated least-squares planes for $[Zn^{II}((5\text{-MeimidH})_2DAP)](BF_4)_2$, Table S-VI, listing temperature-dependent NMR data for $[Zn^{II}((5\text{-MeimidH})_2DAP)]^{2+}$, $[Zn^{II}((imidH)_2DAP)]^{2+}$, and $[Zn^{II}((py)_2DAP)]^{2+}$ in CD_3CN and acetone-d_6, $[Cu^{I}((5\text{-MeimidH})_2DAP)]^{+}$ in CD_2Cl_2 and CD_3CN, and $[Cu^{I}((imidH)_2DAP)]^{+}$ in CD_3CN, Figure S-1, showing the package diagram for $[Zn^{II}((5\text{-MeimidH})_2DAP)](BF_4)_2$, and Figure S-2, giving the simulated ^1H NMR spectrum of the methylene region for $[Cu^{I}((py)_2DAP)]^{+}$ (20 pages); Table S-I, listing observed and calculated structure amplitude factors (×10) for $[Zn^{II}((5\text{-MeimidH})_2DAP)](BF_4)_2$ (20 pages). Ordering information is given on any current masthead page.

Contribution from the Department of Chemistry and Laboratory for Biochemical and Genetic Engineering, William Marsh Rice University, P.O. Box 1892, Houston, Texas 77251, and Departments of Chemistry, University of Notre Dame, Notre Dame, Indiana 46556, and Auburn University, Auburn, Alabama 36849

An Electron Self-Exchange Study of the Coordination-Number-Invariant Pentacoordinate Copper(I/II) Couple $[Cu^{I,II}((5\text{-MeimidH})_2DAP)]^{+/2+}$ [1]

DeAnna K. Coggin,[2] Jorge A. González,[2] Alan M. Kook,[2] Carmen Bergman,[3] Theodore D. Brennan,[3] W. Robert Scheidt,*[,3] David M. Stanbury,*[,4] and Lon J. Wilson*[,2]

Received July 3, 1990

The electron self-exchange rate of the $[Cu^{I,II}((5\text{-MeimidH})_2DAP)]^{+/2+}$ cation couple has been determined in CD_3CN, as a function of temperature, by dynamic NMR line-broadening techniques. Under anaerobic conditions with μ = 25 mM ($(CH_3)_4NBF_4$), the rate constant ranged from 0.8×10^4 (243 K) to 3.5×10^4 M^{-1} s^{-1} (293 K). From the temperature dependence of the self-exchange rate, activation parameters of $\Delta H^* = 16.2 \pm 3.3$ kJ mol^{-1} and $\Delta S^* = -103 \pm 12$ J K^{-1} mol^{-1} have been obtained. An X-ray crystal structure of the $[Cu^{II}((5\text{-MeimidH})_2DAP)]^{2+}$ cation shows the same general pentacoordinate structure as found earlier for the $[Cu^{II}((imidH)_2DAP)]^{2+}$ parent compound, and it is assumed that $[Cu^{I}((5\text{-MeimidH})_2DAP)]^{+}$ is also pentacoordinate as is its Cu(I) parent compound. The present temperature-dependent electron self-exchange data are some of the first such data to be obtained for a synthetic Cu(I/II) couple that remains coordination-number-invariant (CN = 5) during electron transfer. The present electron self-exchange rate constant, together with those for two other, related coodination-number-invariant Cu(I/II) couples ($[Cu^{I,II}((imidH)_2DAP)]^{+/2+}$ and $[Cu^{I,II}((py)_2DAP)]^{+/2+}$) indicate a possible relationship between intramolecular conformational mobility in the Cu(I) partner complex and the electron self-exchange rate of the Cu(I/II) couple. Because of its coordination-number invariance, this small-molecule system resembles the situation at the active site in the blue copper protein plastocyanin (CN = 4) and possibly azurin. It is noteworthy that azurin has a much greater ΔH^* for electron exchange than does the present synthetic system. Crystal data for $[Cu^{II}((5\text{-MeimidH})_2DAP)](BF_4)_2 \cdot {}^1/_2CH_3OH$, $CuF_8O_{0.5}N_7B_2C_{21.5}H_{29}$: a = 11.983 (4) Å, b = 10.360 (4) Å, c = 12.906 (6) Å, α = 68.51 (3)°, β = 73.63 (3)°, γ = 67.06 (3)°, Z = 2, triclinic, space group $P\bar{1}$. A total of 7592 observed data were collected at −155 ± 5 °C and used in the solution. The pentacoordinate cation is disordered into two enantiometric forms around the copper(II) ion. The structures are closer to idealized trigonal bipyramidal than square pyramidal. Crystal data for $[Cu^{II}((imidH)_2DAP)](BF_4)_2$, $CuF_8N_7B_2C_{19}H_{23}$: a = 12.431 (9) Å, b = 14.024 (6) Å, c = 14.296 (11) Å, β = 104.45 (6)°, Z = 4, monoclinic, space group $P2_1/c$. A total of 1358 observed data were obtained. The structure of the cation (as its BF_4^- salt) is more square pyramidal than that of the perchlorate salt whose structure had been previously determined.

Introduction

Unlike heme iron and iron–sulfur electron-transfer proteins, cuproproteins have no extrudable coordination complex, since the active-site structure exists only through chelation of the copper ion with protein residues.[5] Therefore, the study of small-molecule copper complexes (i.e., model compounds) provides one of the only means by which the active-site contribution to electron transfer can be evaluated. For plastocyanin of the blue copper family of electron-transfer proteins, modeling of the active site requires a retained geometry and coordination number (CN = 4) about the metal center during electron transfer and the assurance of an outer-sphere mechanism. Such restrictions are not trivially accommodated in designing synthetic systems for study, since copper is known for its high kinetic lability and its tendency to adopt different coordination geometries and numbers in the +1 and +2 oxidation states. Additionally, an ideal model compound ligand for plastocyanin would present an (N_2SS^*) donor atom set similar to that observed at the active site of the protein. The most common approach toward modeling blue copper active sites has been the design of multidentate ligands with S and N donor atoms,[6-13] but

(1) Taken in part from: Coggin, D. K. Ph.D. Dissertation, Rice University, 1990.
(2) Rice University.
(3) University of Notre Dame.
(4) Auburn University.
(5) Solomon, E. I. In *Copper Coordination Chemistry: Biochemical & Inorganic Perspectives*; Karlin, K. D.; Zubieta, J., Eds.; Adenine Press: Guilderland, NY, 1983; pp 1-22.
(6) Goodwin, J. A.; Stanbury, D. M.; Wilson, L. J.; Eigenbrot, C. W.; Scheidt, W. R. *J. Am. Chem. Soc.* **1987**, *109*, 2979-2991.
(7) Goodwin, J. A.; Bodager, G. A.; Wilson, L. J.; Stanbury, D. M.; Scheidt, W. R. *Inorg. Chem.* **1989**, *28*, 35-42.
(8) Goodwin, J. A.; Wilson, L. J.; Stanbury, D. M.; Scott, R. A. *Inorg. Chem.* **1989**, *28*, 42-50.
(9) Korp, J. D.; Bernal, I.; Merrill, C. L.; Wilson, L. J. *J. Chem. Soc., Dalton Trans.* **1981**, 1951-1956.
(10) Martin, M. J.; Endicott, J. F.; Ochrymowycz, L. A.; Rorabacher, D. B. *Inorg. Chem.* **1987**, *26*, 3012-3022.

0020-1669/91/1330-1125$02.50/0